Structure and properties of gradient PVD coatings deposited on the sintered tool materials

L.A. Dobrzański*, L.W. Żukowska
Institute of Engineering Materials and Biomaterials, Silesian University of Technology, ul. Konarskiego 18a, 44-100 Gliwice, Poland
* Corresponding author: E-mail address: leszek.dobrzanski@polsl.pl

Abstract

Purpose: *Investigate the structure and properties of sintered tool materials, including cemented carbides, cermets and oxide ceramics deposited with single-layer and gradient coatings (Ti,Al)N and Ti(C,N), and to determine the dependence between the substrate type, coating material or linear variation of chemical composition and the structure and properties of the obtained tool material.*

Design/methodology/approach: *Analysis of the structure (SEM, TEM), analysis of the mechanical and functional properties: surface roughness, microhardness tests, scratch tests, cutting tests. The Ti(C,N) and (Ti,Al)N gradient coating was investigated by XPS and AES method. X-ray qualitative phase analysis and the grazing incidence X-ray diffraction method (GIXRD) was employed to collect the detailed information about phase composition of investigated material's surface layer. Computer simulation of stresses was carried out in ANSYS environment, using the FEM method and the experimental values of stresses were determined basing on the X-ray diffraction patterns.*

Findings: *Results of the investigation the influence of PVD coatings structure (single-layer or gradient) and kind on properties of coated tool materials. Coatings are characterized by dense, compact structure. The coatings were deposited uniformly onto the investigated substrate materials and show a characteristic columnar, fine-graded structure. The coatings deposited onto the investigated substrates are characterised by good adhesion and causes increasing of wear resistance. Gradient coatings are characterized by a linear change of chemical composition in the direction from the substrate to the coating surface. A more advantageous distribution of stresses in gradient coatings than in respective single-layer coatings yields better mechanical properties, and, in particular, the distribution of stresses on the coating surface has the influence on microhardness, and the distribution of stresses in the contact area between the coating and substrate has the influence on the adhesion of coatings.*

Practical implications: *Deposition of hard, thin, gradient coatings on materials surface by PVD method features one of the most intensely developed directions of improvement of the working properties of materials.*

Originality/value: *The grazing incidence X-ray diffraction method (GIXRD) and using the XPS and AES method in the investigated coatings were used to describe the gradient character of the coatings. The computer simulation is based on the finite element method, which allows to better understand the interdependence between parameters of process and choosing optimal solution.*

Keywords: *Materials; Tool materials; Gradient coatings; PVD; Finite Element Method*

Reference to this paper should be given in the following way:

L.A. Dobrzański, L.W. Żukowska, Structure and properties of gradient PVD coatings deposited on the sintered tool materials, in L.A. Dobrzański (ed.) Effect of casting, plastic forming or surface technologies on the structure and properties of the selected engineering materials, Open Access Library, Volume 1, 2011, pp. 187-234.

1. Introduction

The development of material engineering and connected with it application of new structural materials of raised strength properties, improved wear resistance and to high temperature, or to the impact exerted by erosion or corrosion factors is effected by continually rising operating requirements involving the present-day machine design technology [1-10, 31,35,55,60].

In view of the fast development of civilization, continuous production growth and incessant crave to improve the quality of the manufactured products, the requirements involving the applied machining tool materials are becoming progressively higher. Tool materials are facing a considerable challenge to ensure appropriate hardness, wear resistance and very good strength properties. The main groups of tool materials, such as high speed steel, cemented carbides, cermets, tool ceramics and also superhard materials, are being constantly improved, either through the modification of their chemical composition or through the constructional optimization of the tool itself [1,2,40-53,55,56,59].

Equally important is the development of tool materials with respect to the fabrication of thin coatings resistant to wear in PVD and CVD processes. It is of considerable importance, since through the selection of appropriate components, we can obtain a tool material of better

properties. This area of tool material development is a priority nowadays, since it is the main route leading to the acquisition of machining tools of suitable properties [1,54,64,69,62].

The improvement of the functionality properties of the tools and the reduction of ecological hazards can be effected through the application of the technology of hard gradient coatings deposited on the tools in PVD processes, principally by ensuring better conditions of tribological contact in the machining area and by eliminating cutting tool lubricants. The machining process is becoming so common that it is necessary to intensify research studies concerning not only the selection of appropriate material for tools but also the deposition technology of modern coatings resistant to wear to cover the material, primarily such as gradient coatings, and to elaborate them and verify in industrial conditions. The application of physical vapour deposition PVD for the acquisition of gradient coatings of high wear resistance, also in high temperatures, enables to improve the properties of these materials in machining conditions, among others through the reduction of friction factor, rise of microhardness, improvement of tribological contact conditions in the contact area tool-machined item, and also to protect these materials against adhesive or diffusive wear and against oxidation [9,40-42,55-58,63,69].

In the Division of Materials Processing Technology, Management and Computer Techniques in Material Science of the Institute of Engineering Materials and Biomaterials of the Silesian University of Technology research studies have been carried out for several years on various applicability aspects of coatings deposited in the PVD process. The crucial part of the research involves the studies concerning the deposition of thin, wear resistant coatings in the PVD processes on the substrate from high speed steels, both sintered and conventional, of economically selected chemical composition, on cemented carbides and cermets, applied in machining tools and other tools, among others for the processing of polymer materials characterized by high abrasion wear resistance or erosion, as well as the studies on PVD coatings deposited on substrate from oxide [52-55,60], nitride and sialon ceramics with the required resistance to abrasive and operating wear. The carried out investigation studies involve wear resistant PVD coatings deposited on substrates from sintered tool materials having single-, two- several-, and multilayer structures [11-39,48,49,64,65]. A lot is to be expected from gradient coatings being a midway link between the single-layer and multilayer coatings. What makes the gradient coatings exceptional is the possibility to easily regulate the wide spectrum of their functionality properties (from mechanical through anti-corrosion and thermal to decorative ones) by changing the dosage proportions of reactive gases or sputtering intensity of particular shields during PVD processes [5,16,17,31-39,45,46,52,54,57,60,62].

The main objective of the present paper is to investigate the structure and properties of sintered tool materials, including cemented carbides, cermets and oxide ceramics deposited with single-layer and gradient coatings (Ti,Al)N and Ti(C,N), and to determine the dependence between the substrate type, coating material or linear variation of chemical composition and the structure and properties of the obtained tool material.

2. Methodology of research

The research studies were carried out on sintered tool materials, such as cemented carbides, cermets and oxide ceramics, deposited and non-deposited with single-layer and gradient coatings resistant to abrasion of the type (Ti,Al)N and Ti(C,N), using the cathodic arc evaporation method (CAE). The characteristics of the investigated materials are presented in Fig. 1 and Table 1.

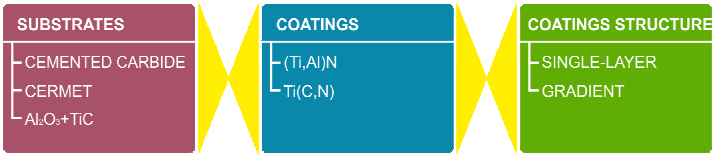

Figure 1. *Characteristics of the investigated materials*

The PVD deposition process of single-layer and gradient coatings of the type (Ti,Al)N and Ti(C,N) was carried out in the Institute of Engineering Materials and Biomaterials of the Silesian University of Technology at Gliwice, on the apparatus DREVA ARC400 of the German Company VTD Vakuumtechnik. The apparatus is equipped with three independent sources of metal vapours.

Before the deposition of coatings, the substrates were prepared for the deposition. The preparation process consisted of two stages. The first stage was carried out outside the operating chamber of the coating apparatus. The multi-point inserts were subjected to chemical cleaning, using washing and rinsing in ultrasonic washers and cascade cleaners, and then they were dried in the stream of hot air. The second preparation stage was carried out in the vacuum chamber of the PVD coating apparatus. That stage consisted in heating the substrate to the temperature of around 400°C with a beam of electrons emitted from the hollow cathode in argon atmosphere with lowered pressure, and then in ionic cleaning using Ar ions with the polarization voltage of the substrate of -300V for 25 minutes.

Table 1. *Characteristics of the investigated materials*

Substrate	Coating	Coating thickness, µm	Roughness, R_a, µm	Micro-hardness, HV	Critical Load, L_c, N	Tool life t, min
Cemented carbide*	uncoated	-	0.13	1755	-	2.5
	(Ti,Al)N	2.2	0.14	2750	52	20.0
	gradient (Ti,Al)N	2.6	0.14	3000	56	25.5
	Ti(C,N)	1.5	0.13	2600	44	5.0
	gradient Ti(C,N)	2.7	0.11	2850	64	5.0
Cermet**	uncoated	-	0.06	1850	-	2.5
	(Ti,Al)N	1.5	0.13	2900	54	19.5
	gradient (Ti,Al)N	3.0	0.12	3150	63	22.0
	Ti(C,N)	1.5	0.12	2950	42	8.0
	gradient Ti(C,N)	2.6	0.11	2950	60	9.5
Al_2O_3+TiC***	uncoated		0.10	2105	-	12.5
	(Ti,Al)N	1.6	0.27	3170	53	21
	gradient (Ti,Al)N	3.2	0.24	3200	65	40
	Ti(C,N)	1.3	0.23	2850	40	15
	gradient Ti(C,N)	2.1	0.21	2950	55	19

***** phase composition: WC, TiC, TaC, Co,
** phase composition: TiCN, WC, TiC, TaC, Co, Ni,
*** phase composition: Al_2O_3, TiC.

For the deposition of coatings, shields of the diameter of 65 mm cooled with water were applied. The shields contained pure Ti and the alloy TiA1 of 50:50% at. The vacuum of 10^{-4} Pa was created in the operating chamber. The coatings were deposited in the atmosphere of inert gas Ar and reactive gases N_2 in order to obtain nitrides, and the mixture of N_2 and C_2H_2 to obtain carbonitride coatings. The gradient concentration change of the chemical composition along the cross-section of the coatings was obtained by changing the dosage proportion of the reactive gases or by changing the intensity of evaporation current of the shield on arc sources.

The surface topography and the structure of the fabricated coatings was investigated at transverse fractures in the scanning electron microscope SUPRA 35 of Zeiss Company, with the accelerating voltage of 10-20 kV and maximum magnification of 60000x. To obtain the images of the structure, the detection of secondary electrons (SE) and back scattered electrons (BSE) was applied. To obtain a brittle fracture of the investigated specimens, notches were cut into their surface with a diamond shield, and then they were broken up after cooling in liquid nitrogen. To improve the conductivity of the investigated material, the specimens were sputtered with carbon using the apparatus JEOL JEE 4B.

The qualitative and quantitative analyses of the chemical composition of the investigated coatings were carried out using the X-ray energy dispersive spectroscopy (EDS), with the application of the spectrometer EDS TRIDENT XM4 of EDAX Company, being a component of the scanning electron microscope Zeiss Supra 35. The research studies were carried out with the accelerating voltage of 20 kV.

The diffraction studies and the observations of thin foil structure were carried out in the transmission electron microscope JEM 3010 UHR of JEOL Company, with the accelerating voltage of 300kV and maximum magnification of 300000x. The diffraction patterns from the transmission electron microscope were being solved using the computer program "ElDyf". Thin foils were made in the longitudinal section, cutting out inserts about 0.5 mm thick from the solid specimens, from which discs of the diameter of 3 mm were cut out, using an ultrasonic erosion machine. Then, such discs were subjected to mechanical rubbing down to the thickness of about 90 µm, and a notch of the depth of around 80 µm was then ground down in the discs. Ultimately, the specimens were subjected to ionic thinning out in the apparatus of Gatan Company.

The changes of chemical concentration of the coating components in the direction perpendicular to its surface, and the concentration changes in the transit zone between the coating and substrate were determined basing on spectroscopic tests: X-ray photoelectron spectroscopy (XPS) and Auger electron spectroscopy (AES). The AES and XPS tests were carried out on the X-ray photoelectron spectrometer of the Physical Electronics Company (PHI 5700/660) whereof diagram is presented in Fig. 2. In this spectrometer the radiation emitted from the anode $A1K_{\alpha}$ (1486.6 eV) was applied.

The maximum resolution of the spectrometer PHI 5700 applied for the measurements was 0.035 eV. The analysis area from which the electrons are collected is selected using the diaphragm for photoelectrons emitted from the investigated specimen, and the smallest area is defined by a circle of the diameter of 30 µm. Through the application of a pumping system, consisting of the ion and sublimation pumps, we can obtain the pressure of 10^{-7}-10^{-8} Pa, referred to as ultrahigh vacuum UHV. The research carried out with the use of the residual gas analyzer RGA of the mass spectrometer demonstrated that the main components of vacuum in the spectrometer are: CO, H_2, CO_2 (given in the order of the highest partial pressures).

Using the XPS technique [3,6], two types of surface were analyzed: immediately after inserting to the spectrometer and after etching with argon ions. In the second case the beam energy was always 4keV for the preset etching times. The analysis of the surface measured immediately after inserting to the spectrometer showed that there are surface impurities, mainly

oxides and a so called aliphatic carbon (various hydrocarbons, carbon oxides). All locations of photoelectron lines were calibrated against binding energy lines of silver $Ag3d_{5/2}$, gold $Au4f_{7/2}$ and copper $Cu2p_{3/2}$. The pure surface of the investigated gradient coatings was obtained in effect of bombarding the specimen with the beam of ions Ar^+ or Xe^+ of the energy of 4.5keV. The analysis involved the lines of titanium Ti2p and carbon C1s [6,15].

In the case of AES analysis [7], the specimen surface was subjected to etching with argon ions of the energy of 4 keV, and the crater formed on the surface was analyzed by means of linear profile. The analyzed elements were selected in accordance with the preset chemical composition of the investigated coatings. The Auger electrons were recorded with the cylindrical mirror analyzer (CMA). The electrons of the prime beam in the AES PHI660 microscope were emitted from the single crystal LaB_6. The accelerating voltage of the electrons was being changed within the range 3-10 kV. In effect of exposing the solid surface to the illumination of the electrons beam, the emission of Auger electrons, secondary electrons and X-ray radiation is taking place. The depth of the Auger electrons analysis is from 0.4 to 5 nm. These electrons are used for the physicochemical analysis of the composition of the investigated surface, whereas the secondary electrons are used for surface imaging with the application of secondary electron microscopy (SEM).

The analysis of phase composition of the substrates and coatings was carried out using the X-ray diffraction method on the X-ray apparatus X'Pert Pro of Panalytical Company, in the Bragg-Brentano system, applying the filtered radiation of cobalt tube at the voltage of 40 kV and filament current of 30 mA. We accepted the step of 0.05° and calculation time of impulses of 10 seconds. Due to the superposition of the reflexes of substrate and coating material and due to their intensity, hindering the analysis of the obtained results, in order to obtain more precise information from the surface layer of the investigated materials, in our further research we applied the grazing incident X-ray diffraction technique with the application of the parallel beam collimator before the proportional detector.

The thickness of the coatings was tested using the calotest method which consists in the measurement of the characteristic quantities of the crater effected by the wear on the surface of the investigated specimen brought about by a steel ball 20 mm in diameter. The space between the rotating ball and specimen surface was being fed with the suspension of diamond grains of the diameter of 1 µm. The test time was accepted at 120 seconds. The measurement of wear extent was carried through the observations on the illumination metallographic microscope LEICA MEF4A. The thickness of the coating was determined on the basis of the following relation:

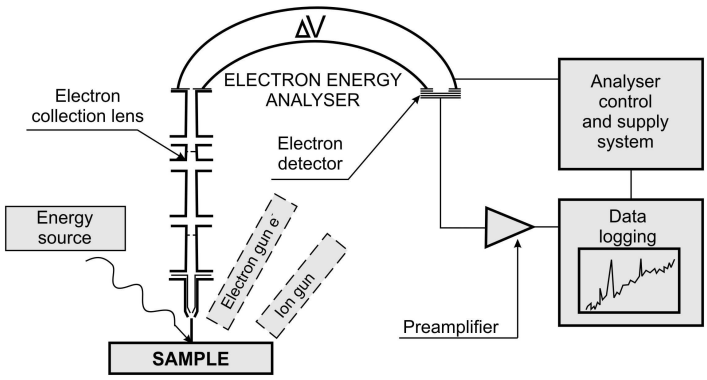

Figure 2. *Schematic diagram of X-Ray Photoelectron Spectroscopy (XPS)*

$$g = \frac{D \cdot (D - d)}{4 \cdot R} \cdot 10^3 \tag{1}$$

where:

g – coating thickness [μm],

D – external diameter of the crater [mm],

d – internal diameter of the crater [mm],

R – ball radius [mm].

In order to obtain average thickness values of the measured coatings, 5 measurements were carried out for each of the investigated specimens. Additionally, to verify the obtained results, the measurements of coating thickness were carried out in the scanning electron microscope at the transverse fractures of the specimens.

The measurements of the surface roughness of the polished specimens without coatings and with deposited coatings were measured in two mutually perpendicular directions on the profilometer Surftec 3+ of Taylor Hobson Company. The accepted measurement length was l=0.8 mm, and measurement accuracy ±0.02 μm. Additionally, to confirm the obtained results, the roughness measurements of specimen surfaces were carried out on the confocal microscope LSM 5 Exciter of Zeiss Company. The parameter Ra was accepted as the quantity describing the surface roughness, in compliance with the Standard PN-EN ISO 4287:1999.

The hardness of the investigated materials was determined using the Vickers method. The hardness of the deposited substrates from sintered tool materials was tested using the Vickers

method with the load of 2.94 N (HV 0.3) in compliance with the Standard PN-EN ISO 6507-1:2007. The tests on microhardness of the deposited coatings were performed on the microhardness meter Future Tech, making use of the Vickers dynamic method. We applied the load of 0.98 N (HV 0.1), enabling, to the highest possible extent, to eliminate the influence of substrate on the obtained results. The measurements were carried out in the mode of periodic loading and unloading, in which the tester loads the indenter with the preset force, maintains the load over some time period and than unloads it. The dynamic hardness is determined from the following equation [11]:

$$DH = \alpha \cdot \frac{P}{D^2} \tag{2}$$

where:
α – a constant allowing for the influence of indenter shape, for Vickers α=3.8584,
P – preset load, mN,
D – imprint depth, μm.

The trial makes it possible to observe the changes of plastic and elastic strain of the investigated material, respectively during the loading and unloading due to a high-precision measurement system which can record the depth of the formed imprint in successive phases of the test. The measurements were carried out making 6 imprints for each of the investigated specimens. An average was determined, as well as standard deviation and confidence interval, assuming the confidence factor at 1-α = 0.95.

The adhesion assessment of the deposited coatings to the investigated sintered tool materials was carried out using the scratch-test on the apparatus REVETST of CSEM Company. The method consists in moving the diamond indenter along the surface at constant speed, with the loading force increasing proportionally with the movement. The tests were carried out for the loading force within the range of 0±100 N, increasing with the speed of (dL/dt)=100N/min along the path of 10 mm.

The critical load Lc at which the coating loses its adhesion was determined basing on the value of acoustic emission (AE) recorded during the measurement and on the observation of scratch lines effected during the scratch-test. The character of the fault was assessed basing on the observations in the scanning electron microscope Zeiss Supra 35 and in the confocal microscope LSM 5 Exciter of Zeiss Company.

The operating properties of the deposited coatings were determined basing on the technological machining trials at room temperature. The tests on cutting ability of the investigated tool materials without coatings and with the deposited coatings were carried out basing on the technological cutting trials without cutting tool lubricants on a universal numerically controlled lathe Gildemeister NEF 320. The cast iron EN-GJL-250 of the hardness of 250 HV was selected as material subjected to machining. For the technological cutting trials, we applied inserts fixed in a universal lathe chuck which ensures the maintenance of geometric parameters of the inserts.

The following parameters were accepted for the cutting ability tests:

- rate of feed f=0.1 mm/rev.,
- turning depth ap=1 mm
- cutting velocity vc=150 m/min.

The durability of the inserts was determined basing on the measurements of wear strip width on the tool flank, measuring the average wear strip width VB after the machining in a definite time interval. The machining trials were being stopped when the VB value exceeded the accepted criterion for after-machining, i.e. VB=0.2 mm. In the case of non-deposited tools, the trial was being carried out until the wear criterion had been reached , and the duration of the trial for the tools with deposited coatings was the same or longer than in the case of non-deposited tools, whereby we can compare the wear strip width VB after the wear criterion has been reached by the non-deposited specimen. The VB measurements were carried out with the application of the illumination microscope Carl Zeiss Jena. The images of tool flank and attack surface of the inserts of different wear degree as well as the topography of the fractured tool with the use of a 3D model were obtained with the application of the scanning electron microscope Zeiss Supra 35 and of the confocal microscope LSM 5 Exciter of Zeiss Company. The analyses of chemical composition in the microareas were carried out using the EDS method. The obtained research results were presented in the form of graphs determining the dependence of wear strip width on the tool flank VB as the function of testing time, assuming the preset conditions of the experiment. Fig. 3 presents the basic tribological faults of the tool material cutting edges, which were then used to assess the wear characteristics of the investigated sintered materials deposited with PVD coatings.

The work presents the application of the finite elements method for the analysis of the distribution of eigen-stresses in the coatings obtained in the PVD process, as dependent on the parameters of the process and the material of the substrate and coating.

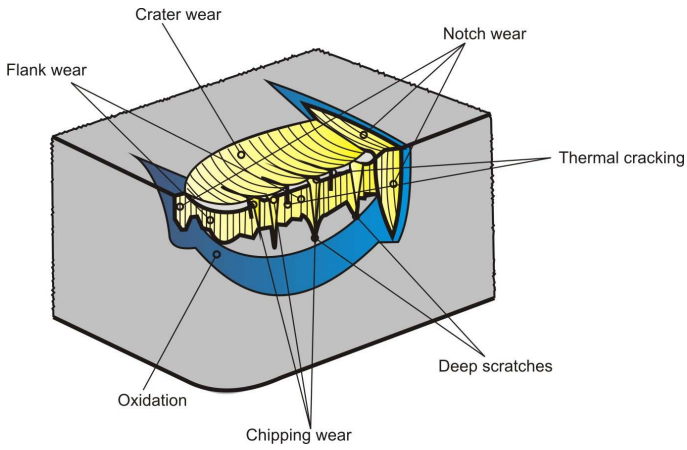

Figure 3. *Tool wear model [1,65]*

The model whereof objective is to determine the eigen-stresses in gradient and single-layer coatings (Ti,Al)N and Ti(C,N) on the substrate from cemented carbides, cermet and oxide tool ceramics, was elaborated using the finite elements method, assuming true dimensions of the specimen. The geometry of the insert with the deposited gradient and single-layer coatings as well as the calculations were carried out using the program ANSYS 12.0. On account of the predicted simulation range, parametric calculation files were elaborated which allowed to perform the analysis in a comprehensive way. We employed the experience involving computer simulation works in material engineering carried out for many years at the Division of Materials Processing Technology, Management and Computer Techniques in Materials Science of the Institute of Engineering Materials and Biomaterials of the Silesian University of Technology [66]. The geometrical model was subjected to discretization with the element of the PLANE 42 type for substrate material and external coating. The element of that type is applied for the modeling of spatial structures with the use of a flat (2-D) element of solids. It can be also applied for the modeling of the structures described by means of axial symmetry. It is a simpler and faster method, by the application of which we can avoid many errors which could have occurred when applying the network on spatial solids. This type of description generates radically smaller MES models as compared to the full 3D description, maintaining the understanding of the general description. The element of PLANE 42 type is defined by four basic nodes and can demonstrate such features as plasticity, creep, swelling, and it also enables the modeling of high bending and tension of the modeled objects. The true model was

subjected to discretization, which is presented in Fig. 4. The calculation model consists of 12816 nodes and 11780 elements. In order to avoid errors in the calculation of eigen-stresses in the coatings, we applied variable quantities of finite elements. In the places where higher gradients of stresses were expected, the network is more condensed than in the areas where the stresses were expected to have values similar to one another. Therefore, in the coatings we applied smaller elements which better reflect the gradients of stresses, and in the substrate material the elements are increasing with the rise of the distance from the coatings.

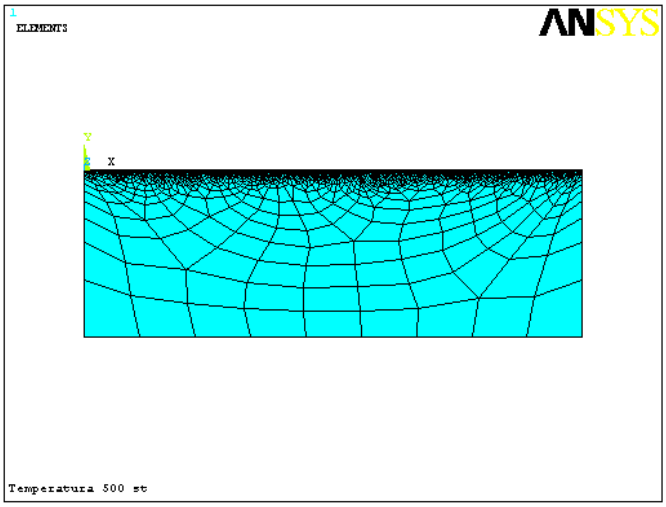

Figure 4. *True model subjected to discretization with deposited gradient and single-layer (Ti,Al)N and Ti(C,N) on different substrates*

Since it was necessary to calculate eigen-stresses in the material of the chemical composition which was changing in the way perpendicular to the surface, the ideographic differentiation of the modeled gradient coatings was carried out into zones corresponding to the areas of similar chemical composition. The model with the spherical division of gradient coating was elaborated in the way ensuring that it was possible to determine the averaged eigen-stresses in the coating areas important in view of the applicability properties and to compare the obtained results with the calculations carried out for homogeneous coatings.

The following boundary conditions were accepted to simulate the eigen-stresses in the gradient single-layer coatings (Ti,Al)N and Ti(C,N) on different substrates:

- the temperature change of the PVD process is reflected by cooling the specimen from 500°C to the ambient temperature of 20°C,
- for the coatings (Ti,Al)N and Ti(C,N) and for the substrate from cemented carbides, cermets and oxide tool ceramics, the material properties were accepted basing on literature data [6] and MatWeb catalogue. The discrepancies in literature data involving the values of physical properties of particular materials result from different acquisition methods, from the differences in the structure and composition of the materials and from errors in the applied measurement method [66],
- the substrate of the investigated specimen is immobilized due to depriving all nodes lying on this axis of all degrees of freedom.

With the temperature drop, from the coating deposition temperature (500°C) to the ambient temperature (20°C), eigen-stresses are generated both in the coating and in the substrate material, connected principally with different thermal expansion of particular materials. The distribution of these stresses is also connected with the geometry of the specimen and with thermal transfer during the cooling process. In effect of non-uniform cooling of the specimen material in the particular areas, the distribution of stresses on the coating surface and their concentration in the corners of the specimen is different.

To verify the results of computer simulation, the values of eigen-stresses in the investigated single-layer and gradient coatings were calculated using the X-ray $\sin^2\psi$ technique.

3. Results

The investigated sintered tool materials are characterized by a well condensed compact structure without pores, and in the case of oxide ceramics Al_2O_3+TiC the topography of the fracture surface bespeaks of high brittleness [24,25], characteristic of oxide ceramic materials (Figs. 5-9).

Basing on the diffraction tests and on the studies involving the structure of thin foils carried out in the transmission electron microscope it was demonstrated that in the investigated substrate materials from cemented carbides and cermets, there are numerous faults of crystalline structure inside the grains of WC and TiC carbides, including dislocations and stacking fault. A part of dislocations is forming low-angle borders dividing the carbide grains into subgrain areas of a small disorientation angle (Figs. 11-12). It was also demonstrated that the average diameter of the wolfram carbide grains is about 1 µm, which places them into the category of fine-grained materials.

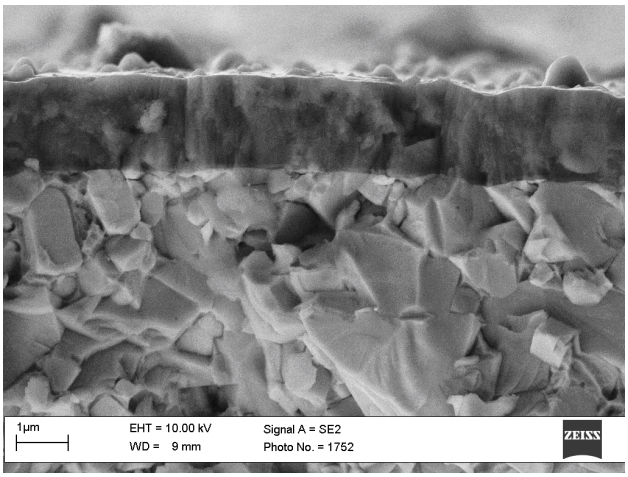

Figure 5. *Fracture surface of the (Ti,Al)N coating deposited onto the cemented carbides substrate*

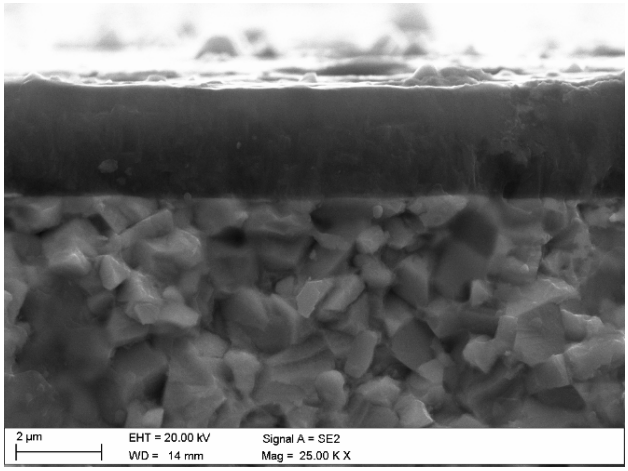

Figure 6. *Fracture surface of the gradient (Ti,Al)N coating deposited onto the cemented carbides substrate*

The results of diffraction tests involving thin foils from the Ti(C,N) coating confirm the occurrence of a phase of the cubic lattice, in compliance with TiN and Ti(C,N). Due to the isomorphism of phases TiN and Ti(C,N) and the similar value of network parameter, it is not possible to differentiate these phases with the electrons diffraction method (Fig. 13). It was also

demonstrated, basing on the tests involving thin foils from the (Ti,Al)N coating that this coating contains principally very fine grains of the crystalline structure corresponding to the phase AlN of the cubic lattice (Fig. 14), and also very few grains of the structure and parameters of AlN phase of the hexagonal lattice. The grains of carbonitrides and of nitrides forming the coating have a very high dislocation density and are very fine – the average grain diameter in the coatings from carbonitrides Ti(C,N) and nitrides (Ti,Al)N does not exceed 0.1 µm.

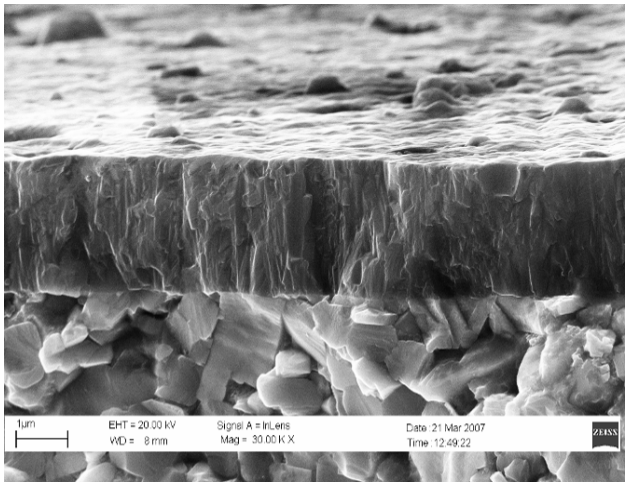

Figure 7. *Fracture surface of the (Ti,Al)N coating deposited onto the cermet substrate*

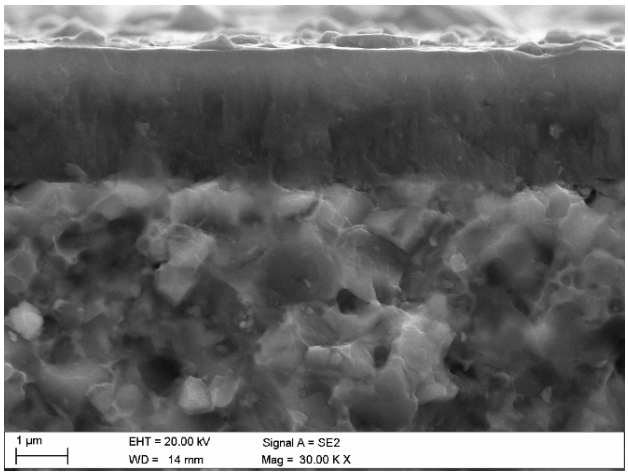

Figure 8. *Fracture surface of the gradient Ti(C,N) coating deposited onto the cermet substrate*

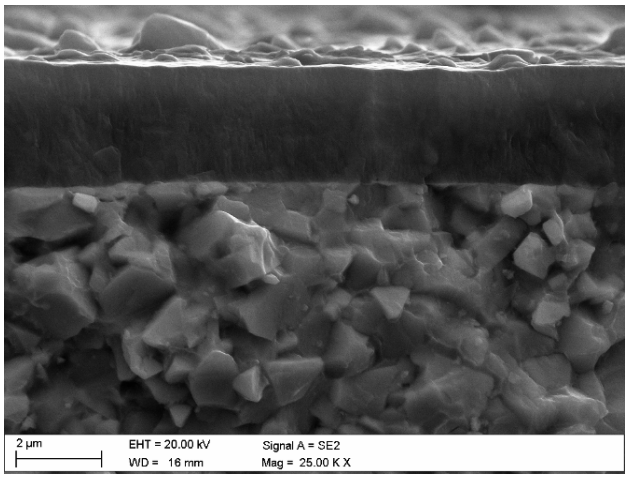

Figure 9. *Fracture surface of the gradient Ti(C,N) coating deposited onto the cemented carbides substrate*

The deposited coatings, both single-layer and gradient ones, have a continuous structure. In the case of gradient coatings, the lines separating particular zones of the coating of the chemical composition different from one another were not determined. It was demonstrated that the coatings are uniformly deposited and are characterized by close adhesion to the substrate, without pores, cracks and discontinuities (Figs. 5-9).

The observations involving the surface morphology of the coatings fabricated in the PVD-CAE process on the substrate from cemented carbides, cermets and oxide ceramics are indicative of high non-homogeneity connected with the occurrence of numerous droplet-shaped microparticles (Fig. 10a). The observed morphological defects brought about during the deposition of the coating are most probably effected by splashing of titanium droplets liberated from the titanium shield onto the substrate surface, which has been confirmed by EDS tests from the microareas (Fig. 10b,c). The droplets observed in SEM assume regular shapes, their size is different and is within the range from the tenths of a micrometer to around a dozen micrometers.

We also observed agglomerates created on the coating surface from several joined microparticles. Furthermore, we observed hollow areas generated in effect of the liberation of titanium microparticles after the termination of the coating deposition process.

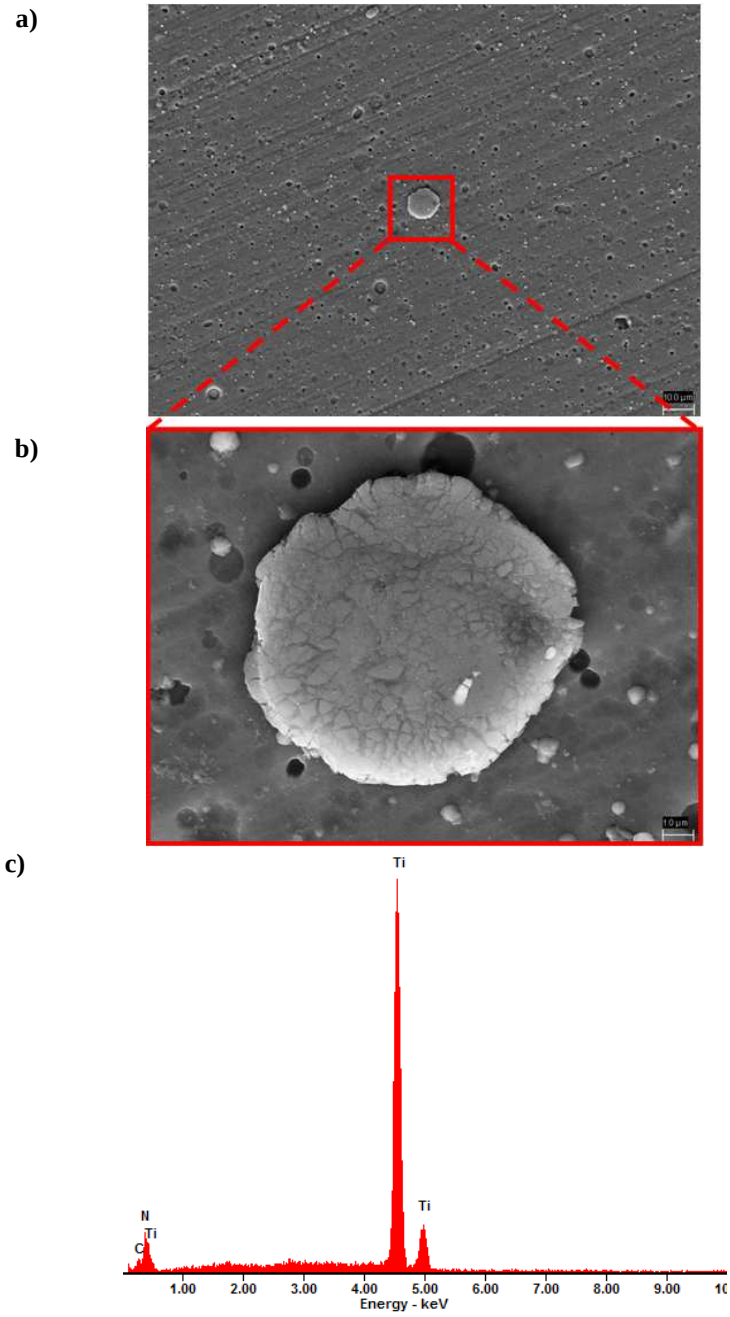

Figure 10. *a,b) Surface topography of the gradient Ti(C,N) coating deposited onto the cermet substrate, c) X-ray energy dispersive plot the area X as in a figure a*

In effect of the carried out research on chemical composition with the use of XPS method, it was demonstrated that the non-etched surface of the coating Ti(C,N) contains small concentration of silicon impurity (around 1% at.) The calculated value of atomic concentration showed that with the fabrication of the coating by means of the PVD method the obtained surface is coated with various adsorbents, mainly carbon oxides and oxygen atoms (Fig. 15). The shape of C1s lines contains at least three components. Two of them are clearly seen at the energy of 284.8 eV and 282.1 eV. The component of the highest intensity, of the energy of 284.8 eV can be ascribed to surface carbon (aliphatic carbon compounds, i.e. hydrocarbons) which does not come from the deposition of Ti(C,N) coating.

The position of lines of lower binding energy of 282.1 eV is typical for carbides. The complex shape of lines observed at the energy of about 288 eV corresponds to carbon oxides adsorbed on the surface of the coating. The intensity of peaks corresponding to surface carbon and carbon oxides is gradually decreasing with the etching time with argon ions. After 20 minutes of etching we can see only one component in the line C1s corresponding to carbides. A similar situation is taking place in the case of titanium lines (Fig. 16). The spectrum of Ti2p lines contains additional components of the doublet. The component of higher binding energy corresponds to titanium atoms in the TiO_2 compound, and the component of lower binding energy corresponds to titanium atoms in the Ti(C,N) coating [60]. After four minutes of etching with argon ions, only one component of the Ti2p doublet is visible. The obtained results for titanium lines and carbon lines demonstrate that the atoms of titanium and carbon are combined with one another in the Ti(C,N) coating in the form of titanium carbide TiC.

In compliance with the accepted assumptions, the deposited Ti(C,N) coating should be characterized by the majority of nitrogen concentration as compared to carbon in the bordering area with the substrate, and by the majority of carbon concentration as compared to nitrogen in the area around the surface. In effect of the analysis of the impurity-free coating surface it was demonstrated that the concentration of the particular components of the coating in the area around the surface is correct (Table 2). A very low atomic concentration of oxygen can be indicative of a low impurity level of the coating with oxygen compounds. Oxygen compounds can be migrating to the inside of the rough coating from residual gases during the PVD process. The obtained ratio of C/N=1.3 is typical for Ti(C,N) coatings. The atomic concentration of carbon with respect to nitrogen atoms in the transit area between the Ti(C,N) coating and substrate should be reversed. But the XPS tests were carried out only to characterize the coating. The investigated specimen was then etched with argon ions for t=50 min, and Fig. 18 presents the depth profile of the chemical composition of the investigated

coating. The oxygen impurity level of the coating is below 2%. The distribution of the particular elements in the investigated coating is maintained at the constant level. The binding energy for the N1s line being 397 eV corresponds to the TiN compound [16].

In effect of etching with argon ions in time t=50 min the depth of the crater did not exceed

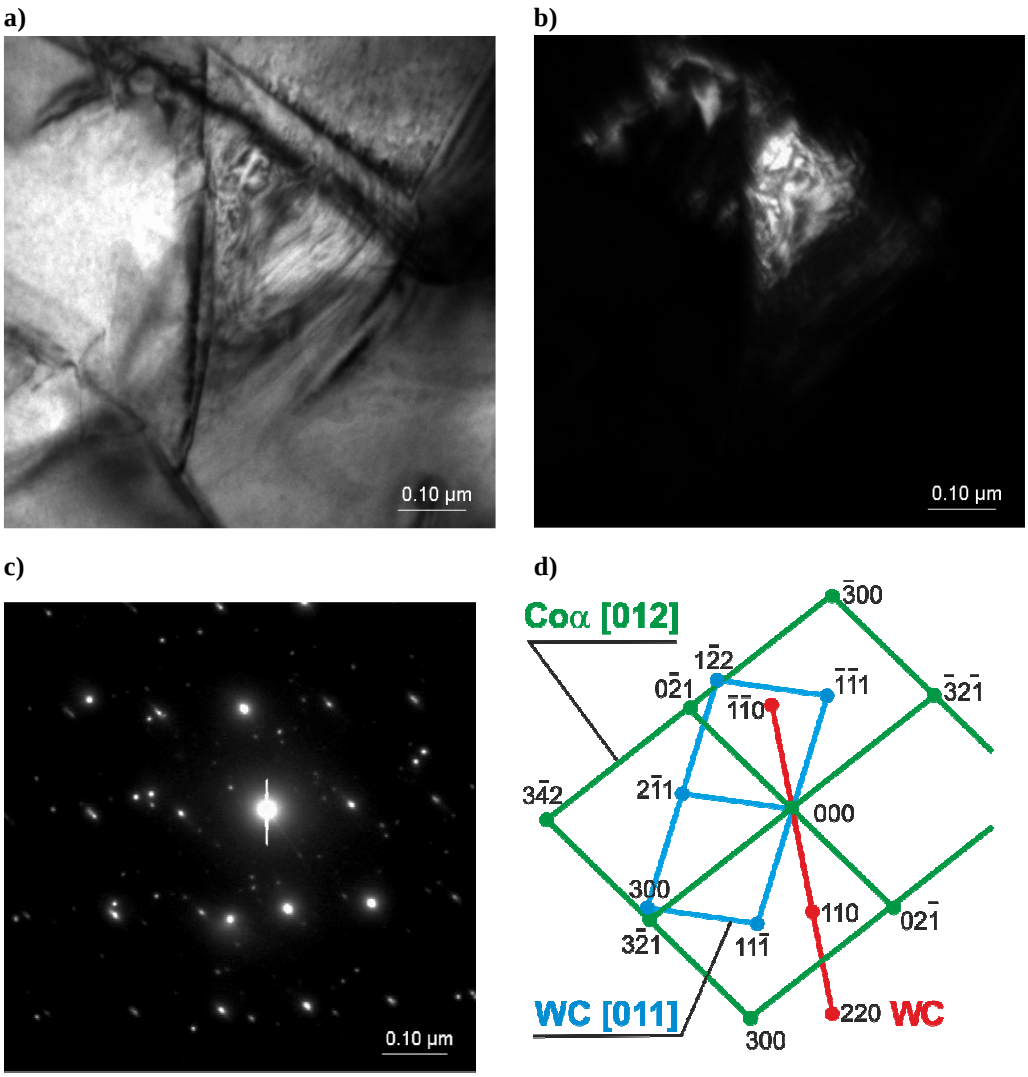

Figure 11. *Structure of cemented carbides substrate: a) bright field; b) dark field from* $(2\bar{1}1)$ *WC reflex; c) diffraction pattern from area b and d) solution of the diffraction pattern*

the range of area around the surface, and therefore the gradient character of the coating could not be observed. In order to investigate the transit area between the investigated coating and substrate, the etching of the investigated specimen with argon ions to the substrate was carried out.

Basing on the tests involving the chemical composition in the coating area with the AES method, the chemical composition of the coating was confirmed, reflecting the assumptions, and at the bottom of the crater generated in effect of etching we found the elements where of the substrate consists of. The diameter of the crater effected by argon ions bombarding is about 500 micrometers and is dependant on the collimation of the incident ions beam and on the set etching area in the applied ionic area.

The transit area between the Ti(C,N) coating and substrate is presented in Fig. 17a,b with the profile of the created crater. The distribution of particular elements present in the transit area is presented in Fig. 17c. The obtained intensities for all elements were recalculated into atomic concentration. Unfortunately, in the Auger electrons spectrum, the nitrogen line overlaps the titanium line [6,7].

The atomic concentration of wolfram in the substrate is at the level of 4%, and the atomic concentration of nickel is 2%. The width of the transit area in the crater is about 200 micrometers. The change of atomic concentration of the elements in the gradient coating is smooth and not step-wise.

In the case of the gradient (Ti,Al)N coating deposited on the substrate from cemented carbides and cermets, a raised concentration of aluminum, titanium and nitrogen can be observed in the area of external coating, and this concentration is decreasing towards the substrate, which is presented by the linear profile of the investigated specimens with the XPS and AES methods. In the Auger electrons spectrum the nitrogen line overlaps the titanium line, and therefore the analysis of this element with the AES method is not possible. Basing on the produced linear profile, using the XPS and AES techniques, of the (Ti,Al)N coating deposited on the substrates from cemented carbides and cermets, the presence of carbon, wolfram and cobalt in the substrate was determined. The concentration of these elements is gradually decreasing in the transit area, and in the coating itself it is at the level from 0 to 10%.

The tests with the use of X-ray qualitative phase analysis method confirm that the substrate from cemented carbides consists of WC and TiC carbides and cobalt matrix (Fig. 19). In the case of cermet, we determined the presence of carbonitride Ti(C,N), TiC and WC carbides and reflexes from Co and Ni. We also confirmed the presence of phases Al_2O_3 and TiC in the substrate from oxide ceramics. Through the application of the X-ray qualitative phase analysis,

we can confirm that on the substrates from cemented carbides, cermets and oxide ceramics Al_2O_3+TiC, the coatings containing the phases (Ti,Al)N, Ti(C,N) were produced in compliance with the assumptions (Figs. 20-21). On the X-ray diffraction patterns obtained with the use of Bragg-Brentano technique, we also determined the presence of the reflexes from the substrate from cemented carbides, cermet and oxide ceramics Al_2O_3+TiC (Figs. 20-21).

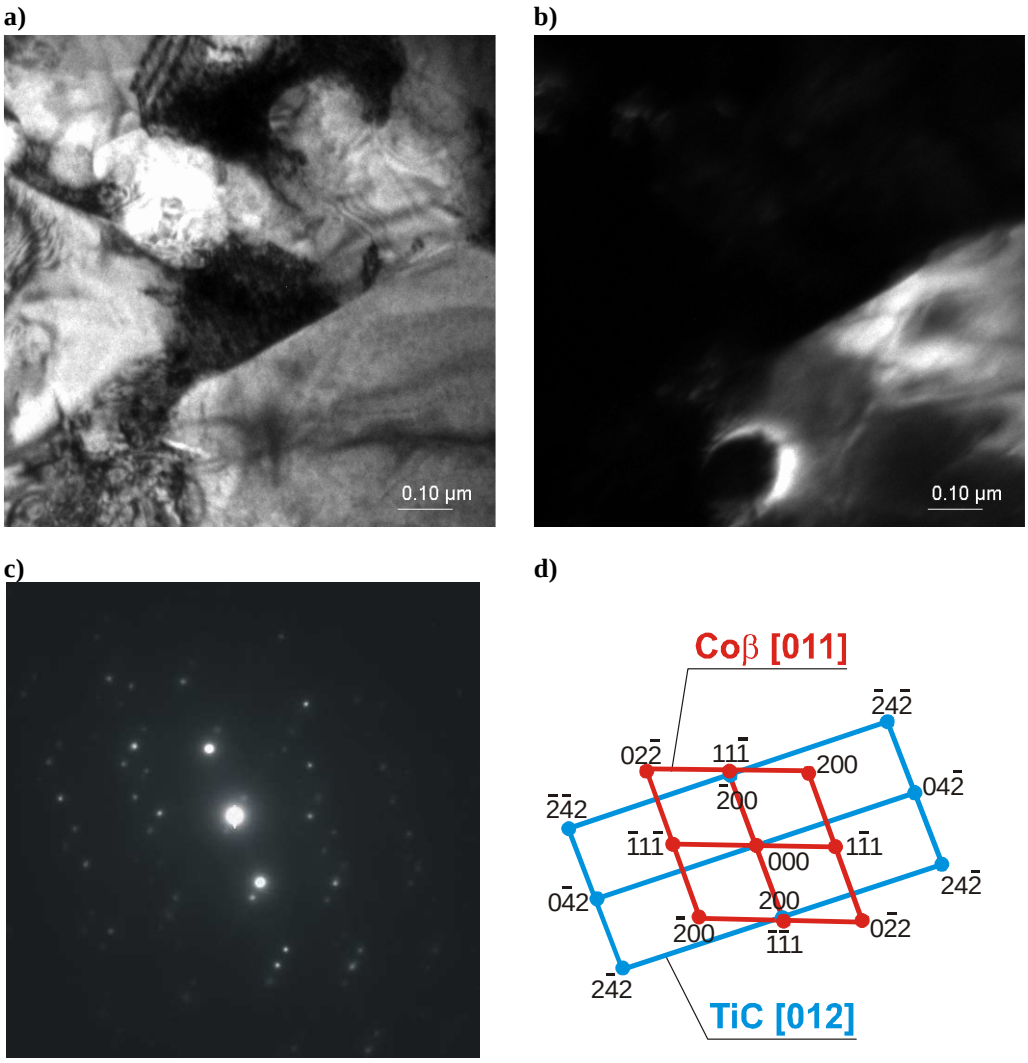

Figure 12. *Structure of cermet substrate: a) bright field; b) dark field from ($\bar{2}00$) TiC i ($11\bar{1}$) Co reflex; c) diffraction pattern from area b and d) solution of the diffraction pattern*

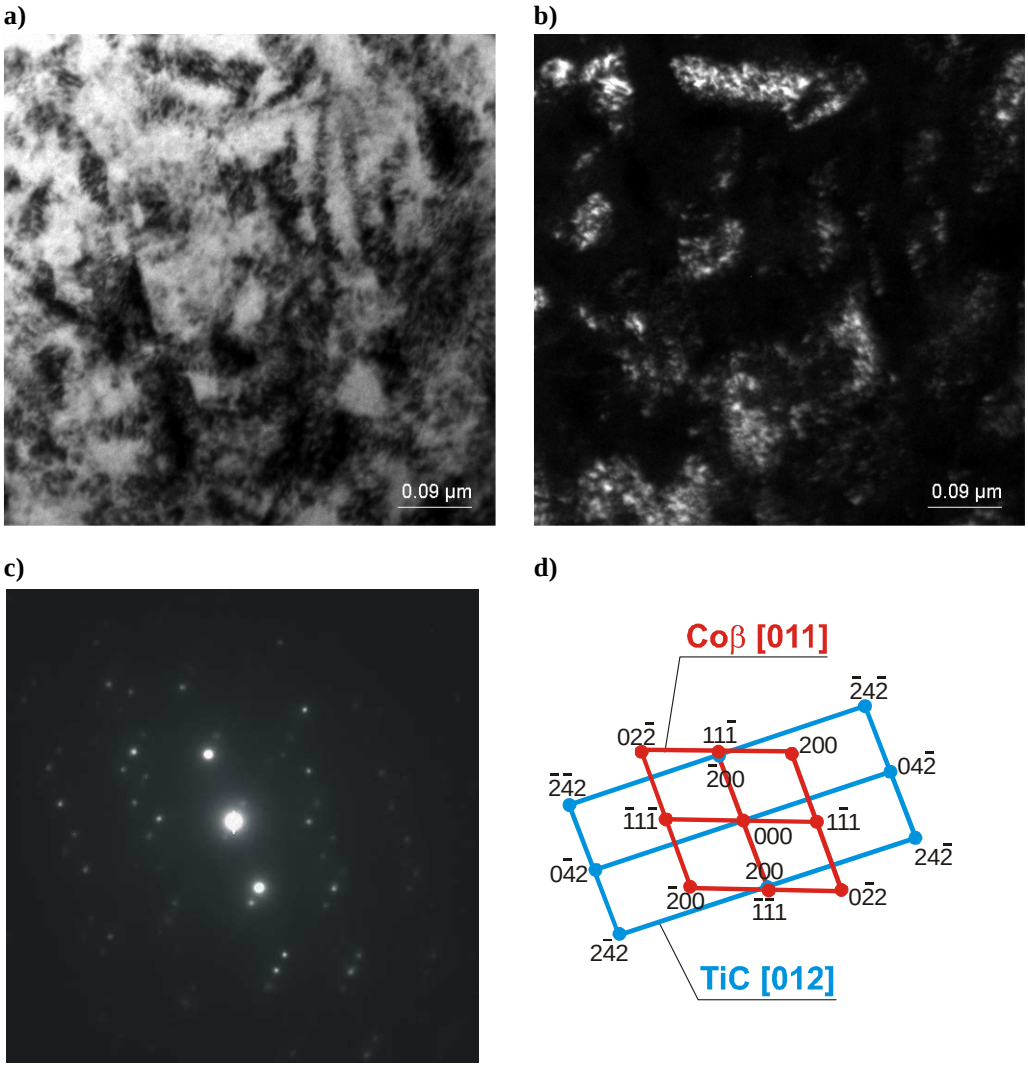

Figure 13. *Structure of Ti(C,N) coating: a) bright field; b) dark field from {111} Ti(C,N) reflex; c) diffraction pattern from area b and d) solution of the diffraction pattern*

Table 2. *Chemical composition of investigated coatings Ti(C,N) on cermet substrates obtained by XPS method*

Element	C	N	O	Ti
Atomic concentration, %	29.9	21.6	4.8	43.7

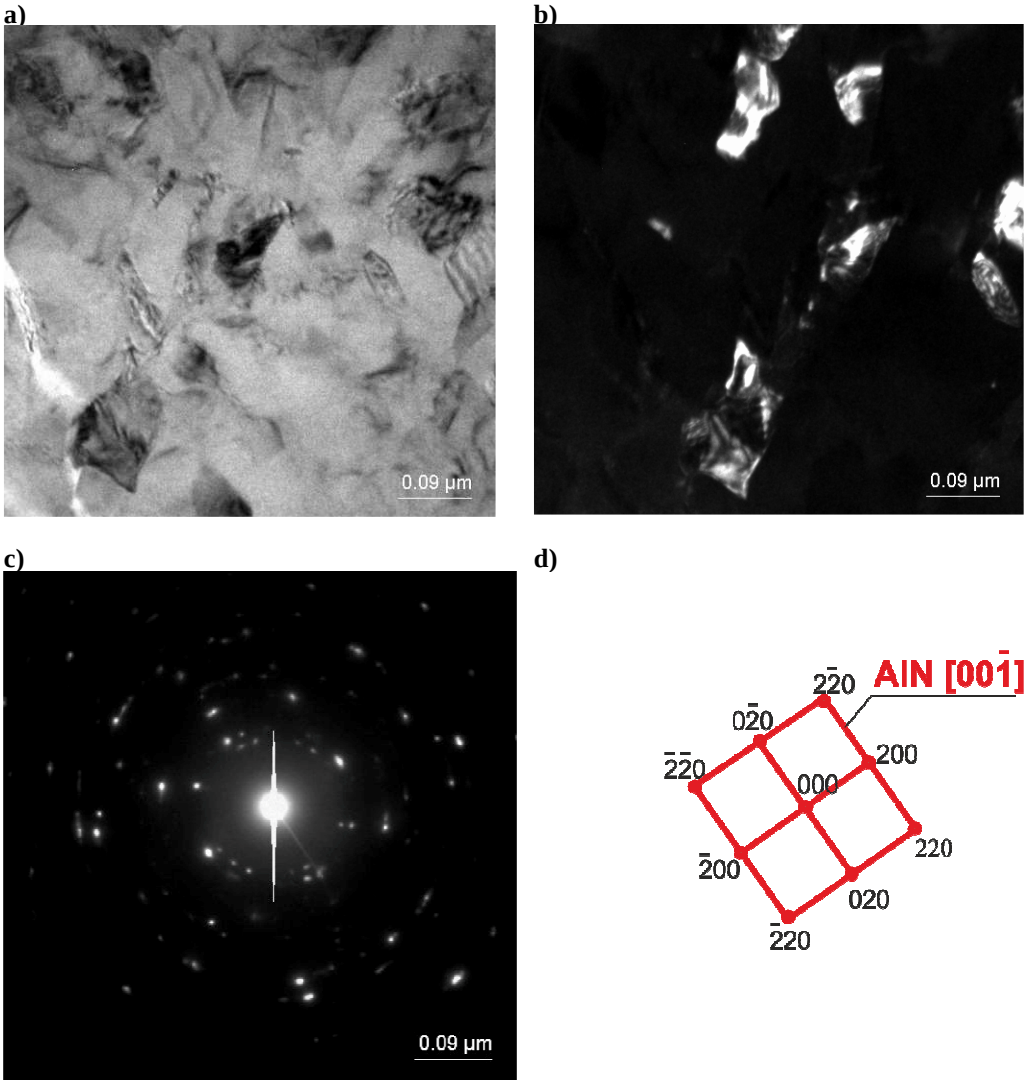

Figure 14. *Structure of (Ti,Al)N coating: a) bright field; b) dark field from ($\bar{2}00$) AlN reflex; c) diffraction pattern from area b and d) solution of the diffraction pattern*

Due to the superposition of the reflexes of the material of substrate and coating and due to their intensity hindering in some cases the analysis of the obtained results, and in order to obtain more precise information from the surface layer of the investigated materials, we applied the SKP or grazing incident X-ray diffraction technique (GIXRD) of the prime X-ray beam (Figs. 22-23).

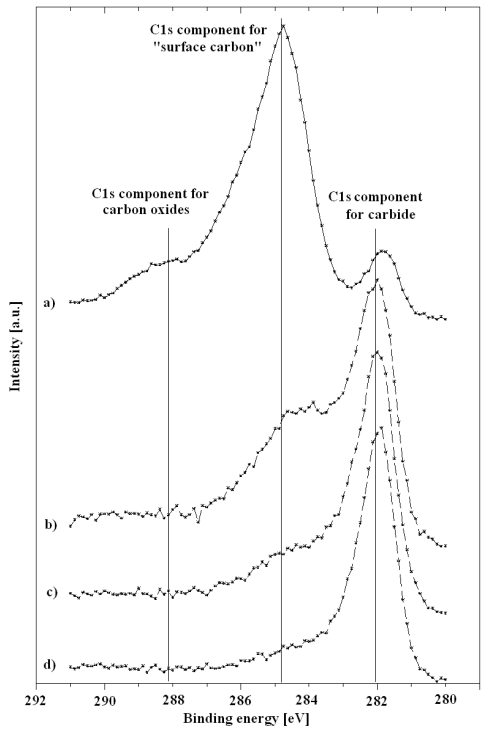

Figure 15. *The shape of C1s lines obtained by XPS method for Ti(C,N) coating: a) "fresh" ex situ surfaces, b) after sputtering Ar^+ ions for t=2 min, c)after sputtering Ar^+ ions for t=4 min, d) after sputtering Ar^+ ions for t=20 min*

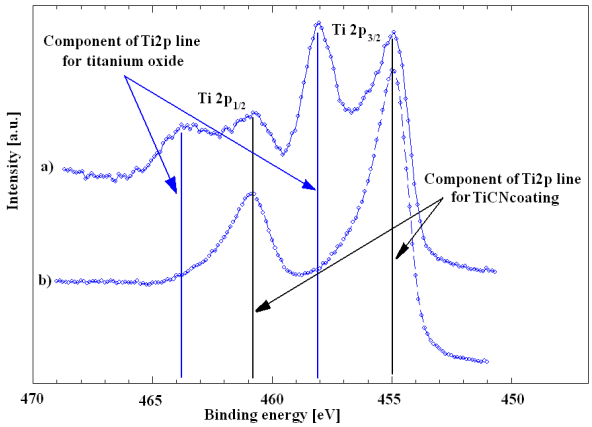

Figure 16. *The shape of Ti2p lines obtained by XPS method for Ti(C,N) coating: a) "fresh" ex situ surfaces, b) after sputtering Ar^+ ions for t=4min*

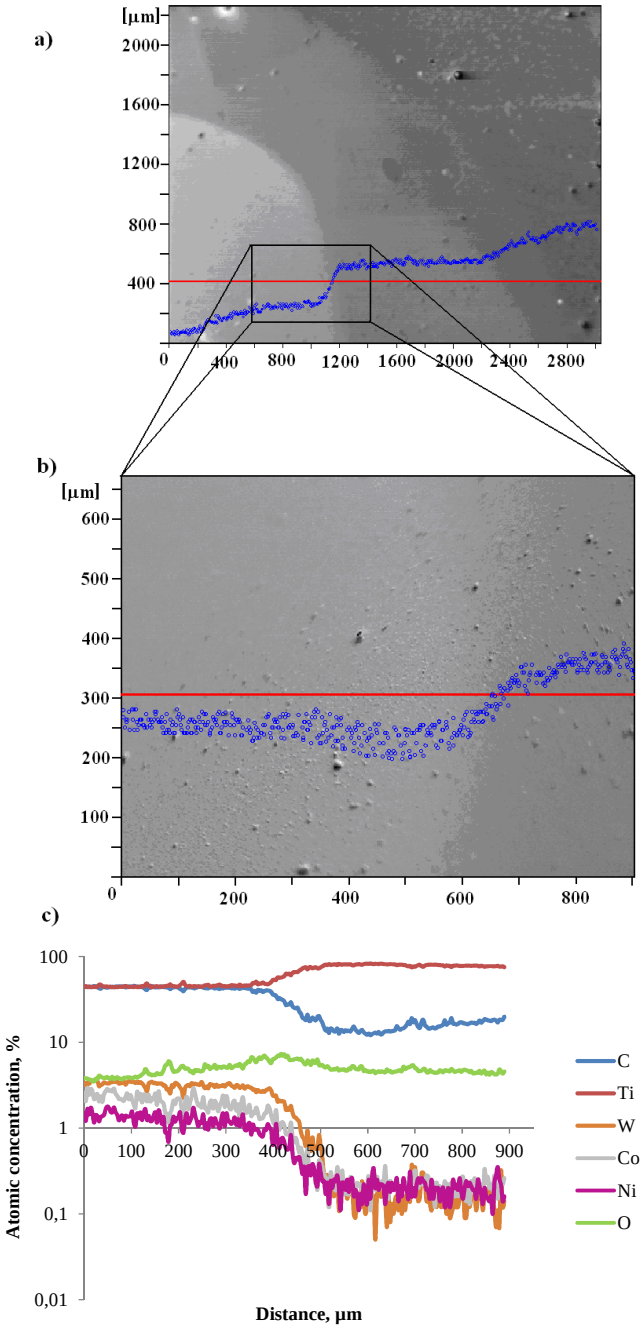

Figure 17. *a,b) SEM picture of transition zone of sputter crater, c) line profile of chemical composition (AES) of gradient Ti(C,N) coating on cermet substrate*

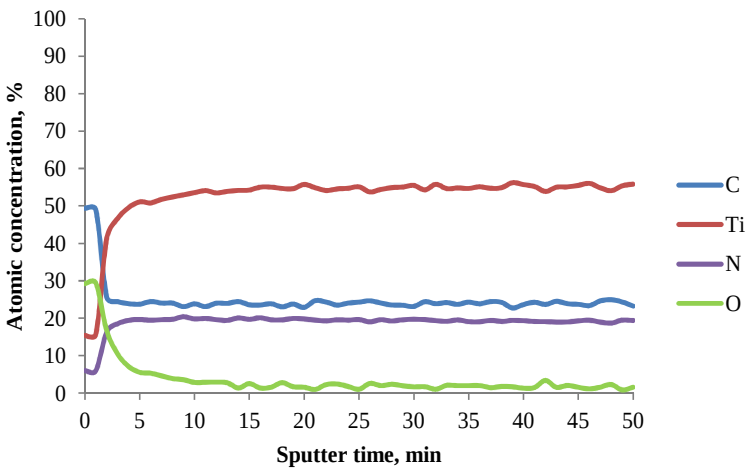

Figure 18. *The distribution of atomic concentration of elements in the surface region of Ti(C,N) coating (XPS)*

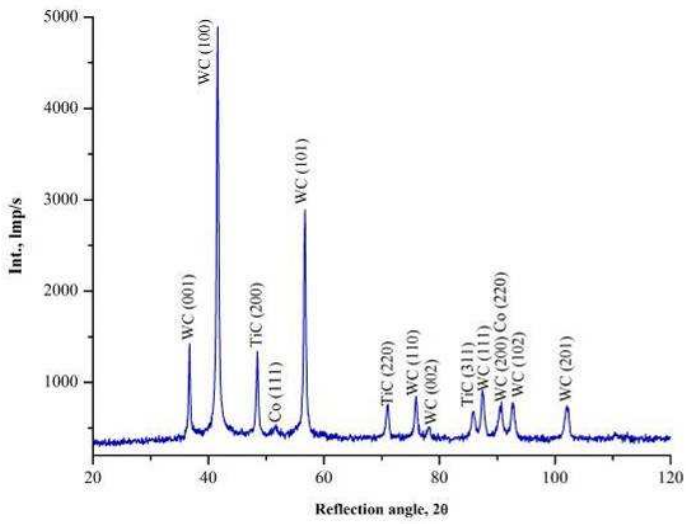

Figure 19. *X-ray phase analysis of the cemented carbides substrate (Bragg-Brentano geometry)*

Basing on the measurement of reflex shift (200) (Fig. 25) in the coating (Ti,Al)N and (111) (Fig. 24) in the coating Ti(C,N) obtained through the grazing incident X-ray diffraction technique (α=1,3, 5, 7) obtained with the use of the proportional detector and the parallel beam

collimator on the side of the bent beam, we determined the network parameters of coatings (Ti,Al)N and Ti(C,N) on the basis of the investigated reflex shift.

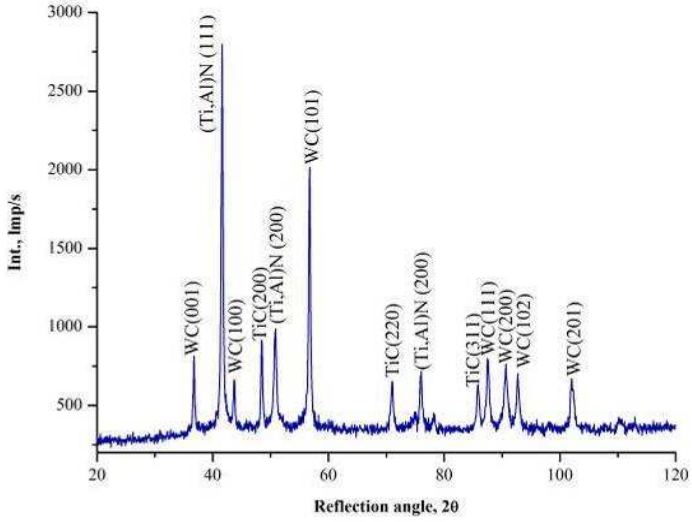

Figure 20. *X-ray phase analysis of the (Ti,Al)N coating (Bragg-Brentano geometry)*

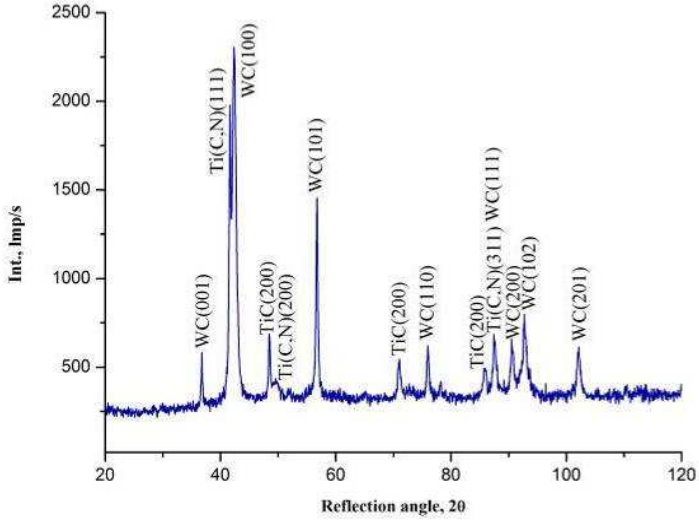

Figure 21. *X-ray phase analysis of the Ti(C,N) coating (Bragg-Brentano geometry)*

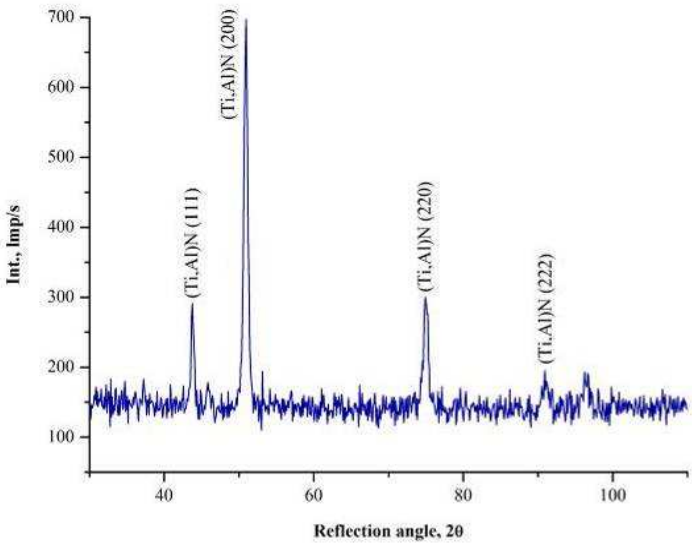

Figure 22. *X-ray phase analysis of the (Ti,Al)N coating (grazing incidence X-ray diffraction GIXRD method), α=1*

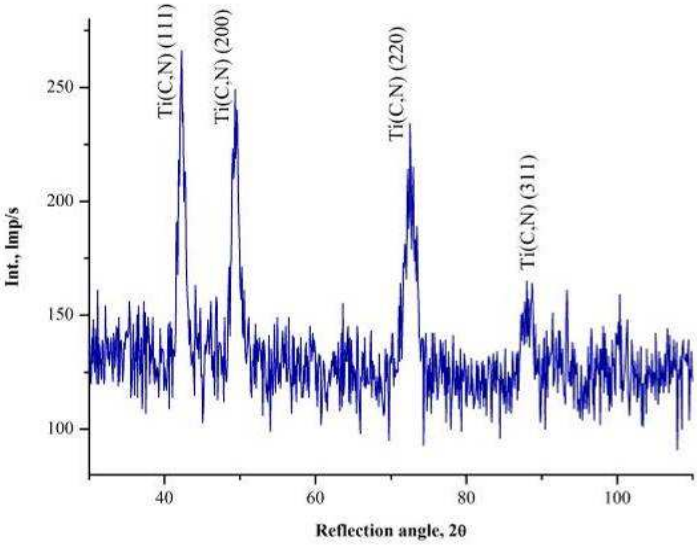

Figure 23. *X-ray phase analysis of the Ti(C,N) coating (grazing incidence X-ray diffraction GIXRD method), α=1*

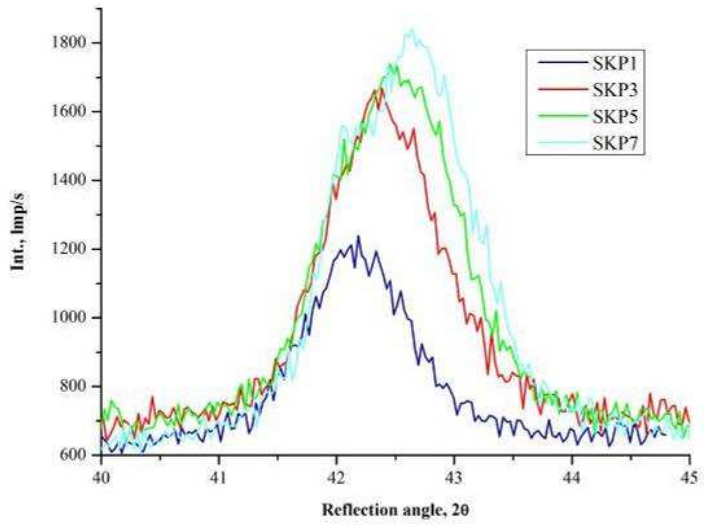

Figure 24. *Change of (111) reflection's position in relation to grazing incidence of the primary beam (Ti(C,N) coating)*

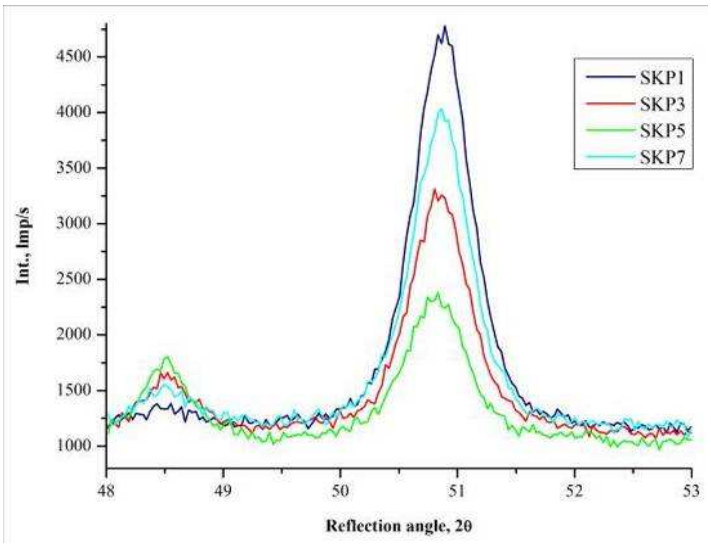

Figure 25. *Change of (200) reflection's position in relation to grazing incidence of the primary beam ((Ti,Al)N coating)*

The experimental results of the X-ray analysis were approximated with the use of a combination of base functions: linear function (adjusting background level) and Voight function (matching the investigated reflexes (Ti,Al)N and Ti(C,N) from the planes (200) and (111). For the determination of base function conditions, the Levenberg-Marquardt algorithm was applied, in which the matching quality was characterized by the function $\chi 2$. The $\chi 2$ function is defined as the sum of the squares of the distance of the experimental results from the values reflected by the determined mathematical model. The parameters of base functions for which the function $\chi 2$ reaches its minimum are indicative of the position of the analyzed reflex on the diffractogram. Basing on the carried out research, in the case of carbonitride coatings, it was determined that the network parameter estimated at the depth of 1µm is close to the one quoted in the JCPDS file (42-1489) to the value corresponding to phase Ti(C,N) richer in carbon. With the rise of the incidence angle of the prime beam, which results in the rise of material volume taking part in the diffraction, the estimated network parameter corresponds to the phase Ti(C,N) richer in nitrogen (42-1488) (Fig. 26). In the case of (Ti,Al)N coating, no considerable changes of network parameter value at the depth of the investigated coating were determined (Fig. 26).

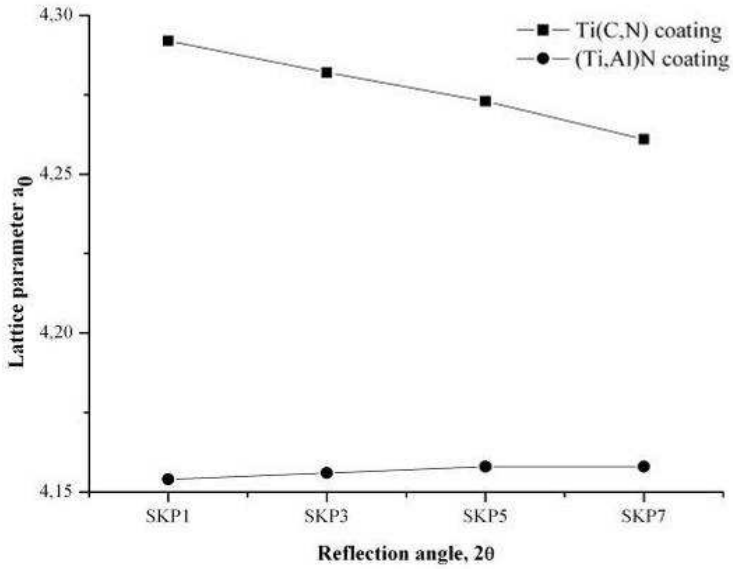

Figure 26. *Comparison of the change of lattice parameter estimated for Ti(C,N) and (Ti,Al)N coating*

The deposition of single-layer and gradient coatings resistant to wear of the type (Ti,Al)N and Ti(C,N) on the investigated sintered tool materials results in the rise of roughness parameter R_a which is within the range from 0.11-0.27µm, and is higher than in the case of material surfaces without coatings (Table 1). The roughness rise of the surfaces of the deposited coatings should be linked to the character of PVD process – physical vapour deposition, which was confirmed by the morphological tests of the surface in the scanning electron microscope (Fig. 10). The roughness of the substrate has the influence on the roughness of the deposited coating and on its structure, as well as on the adhesion of the coating to the substrate (Fig. 27). Too high roughness of the substrate (R_a>0.4) can cause a so called thinning out effect and a generation of coatings of low-compacted structure with numerous surface defects and low adhesion to the substrate. With the application of too smooth substrates (R_a<0.04) we can not ensure a satisfying mechanical anchoring of the increasing coating against the substrate [75,159].

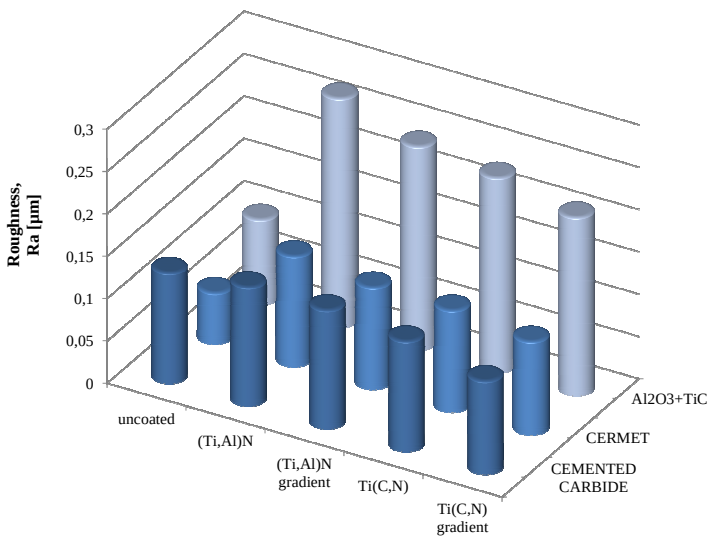

Figure 27. *Comparison of the roughness parameter R_a of the investigated materials*

The deposited PVD coatings are characterized by good adhesion to the substrate within the range L_c=40-65N. In general, the deposition of wear resistant gradient coatings of the type (Ti,Al)N and Ti(C,N) on the investigated sintered tool materials results in a considerable rise of microhardness in the area around the surface (Fig. 28), which, combined with the good

adhesion of the coating to the substrate (Fig. 29) obtained in effect of the application of gradient structure of the coating, yields good functionality properties of these materials, confirmed during machining tests (Table 1).

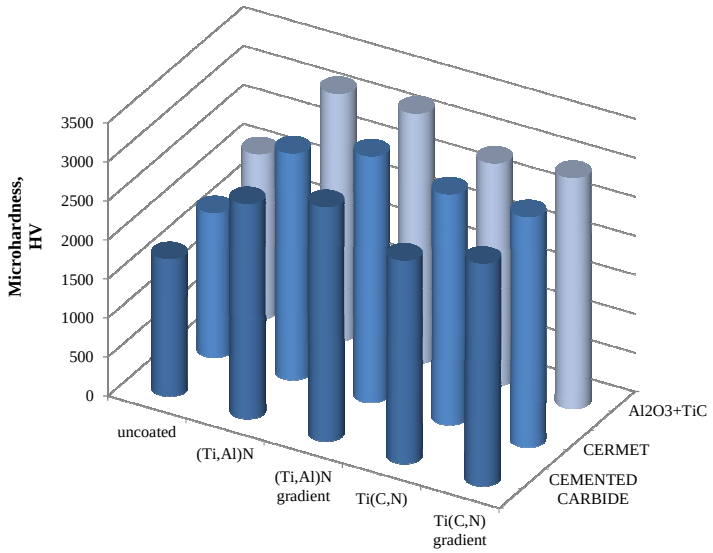

Figure 28. *Comparison of the microhardness of the investigated materials*

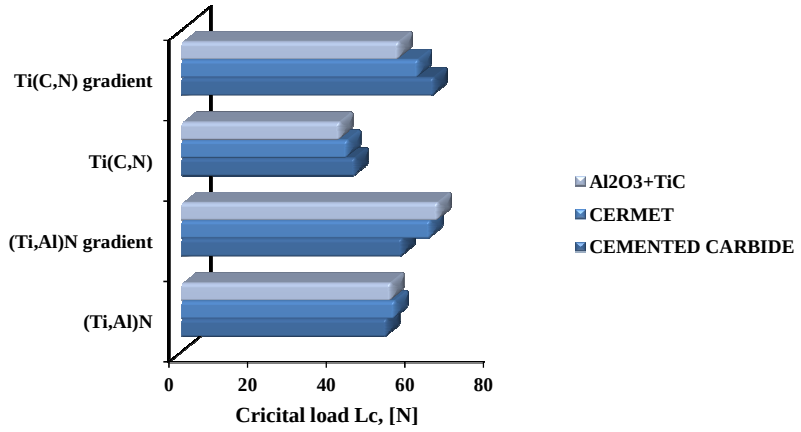

Figure 29. *Comparison of the critical load according to the scratch test of the investigated coating deposited onto cemented carbides, cermets and Al_2O_3 type oxide tool ceramics*

a)

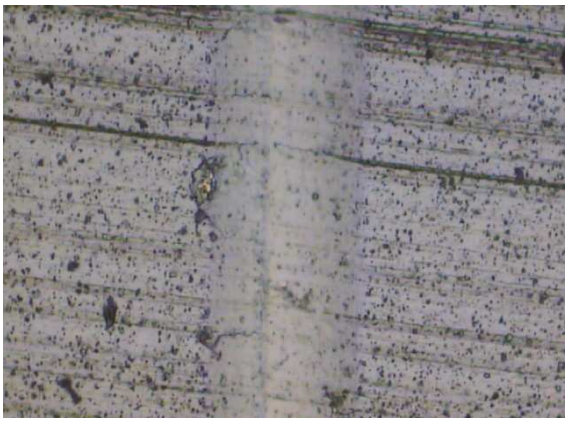

b)

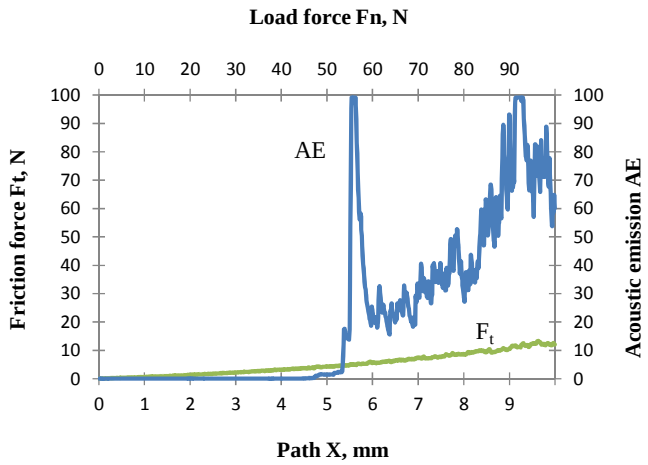

Figure 30. *a) Indenter trace with the optical L_c=45N load (mag. 200x), b) scratch test results of the (Ti,Al)N coating surface deposited on cemented carbides substrate*

The hardness of the substrate material (Table 1, Fig. 28) is 1755 HV for cemented carbides, 1850 HV for cermet and 2105 HV for oxide ceramics. The deposition of the coatings (Ti,Al)N and Ti(C,N) on the investigated sintered tool materials results in a considerable rise of microhardness in the area around the surface within the range of 2600-3200 HV. It was demonstrated that the gradient coatings have higher hardness than the single-layer coatings, independent of the substrate material. Hardness is a property of material dependant on the values of intermetallic bonds, so the hardest materials have covalence bonds, and the rise of the

share of ionic character of the bond is associated with the drop of hardness [11]. Basing on the carried out research it was demonstrated that the hardness of Ti(C,N) coatings, in which the metallic phases TiN and TiC occur, demonstrates lower hardness than (Ti,Al)N coatings in which there are both metallic bonds TiN and covalence bonds AlN. The deposition of the wear resistant coatings on the investigated substrates results in a considerable rise of microhardness of the surface layer, which contributes to lower wear intensity of the cutting edge of machining tools from cemented carbides, cermets and oxide ceramics during the machining process.

a)

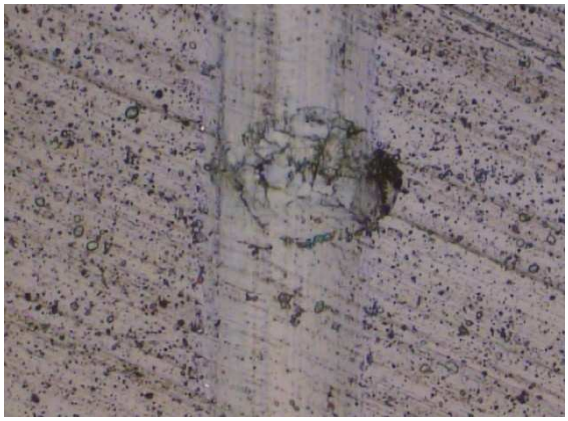

b)

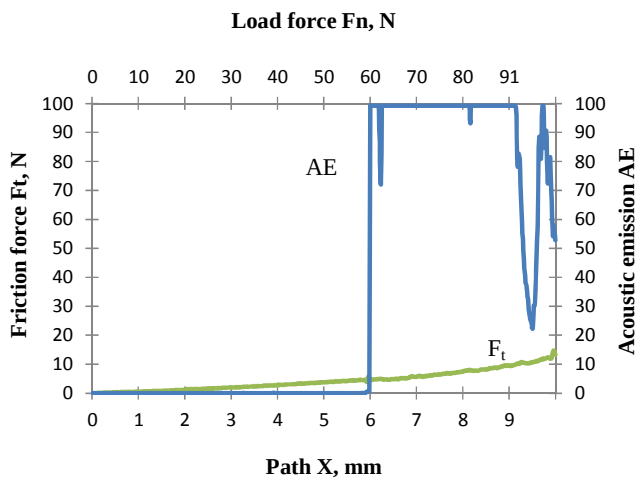

Figure 31. *a) Indenter trace with the optical L_c=59 N load (mag. 200x), b) scratch test results of the gradient Ti(C,N) coating surface deposited on cermet substrate*

In order to check the correlation between the hardness of the investigated materials and the functional properties of the multi-point inserts in the machining tests were carried out, the durability of the inserts was determined on the basis of the measurement of wear width on the flank face after the machining in a definite time interval (Table 1).

The carried out research confirmed that better results are obtained by the tools deposited with (Ti,Al)N coatings, independent of the substrate material. It is connected among others with high microhardness of the coatings and with high wear resistance in raised temperature of the (Ti,Al)N coating. It was also demonstrated that independent of the applied substrate type, higher wear resistance is exhibited by the materials deposited with the gradient coating as compared to the materials deposited with a single-layer coating. It can be related with the reduction of stresses between the coating and substrate in the case of gradient coatings (Table 3), which was also confirmed in the work [54]. Furthermore, it was demonstrated that for the oxide ceramics Al_2O_3+TiC deposited with PVD coatings, the longest durability of cutting edges T=40 min is for the gradient coating (Ti,Al)N and for the single-layer coating (Ti,Al)N T=21 min, as compared to the coatings deposited on cemented carbides and cermets, which can be related with higher hardness of the substrate material (Table 1, Figs. 33-38).

Table 3. *Results of computer simulation of internal stresses in the analysed gradient PVD coatings*

Substrate	Coating	Computer simulation results of internal stress, [MPa]		
		Surface layer	Middle layer	Contact area
Cemented carbide	(Ti,Al)N	-350	-220	130
	Ti(C,N)	-150	160	280
Cermet	(Ti,Al)N	-570	-350	-100
	Ti(C,N)	-300	-50	50
Al_2O_3+TiC	(Ti,Al)N	-380	-250	100
	Ti(C,N)	-170	120	240

The most frequently occurring types of tribological defect indentified in the investigated materials are the mechanical abrasive defects of the flank face, crater formation of the rake face, thermal cracks on the flank face, chipping of the cutting edge (Fig. 39). We also found a build-up of chip fragments of the machined material on the flank face, which is confirmed by the presence of maximums from iron on EDS graphs from the investigated microareas.

The replacement of the single-layer (Ti,Al)N coating with the gradient coating results in a considerable drop of absolute value of eigen-stresses occurring in the material in the contact area between the coating and substrate (Table 3-4), which has a positive influence on the adhesion of gradient coatings to the substrate, which can be one of the main factors yielding better applicability properties such as wear resistance.

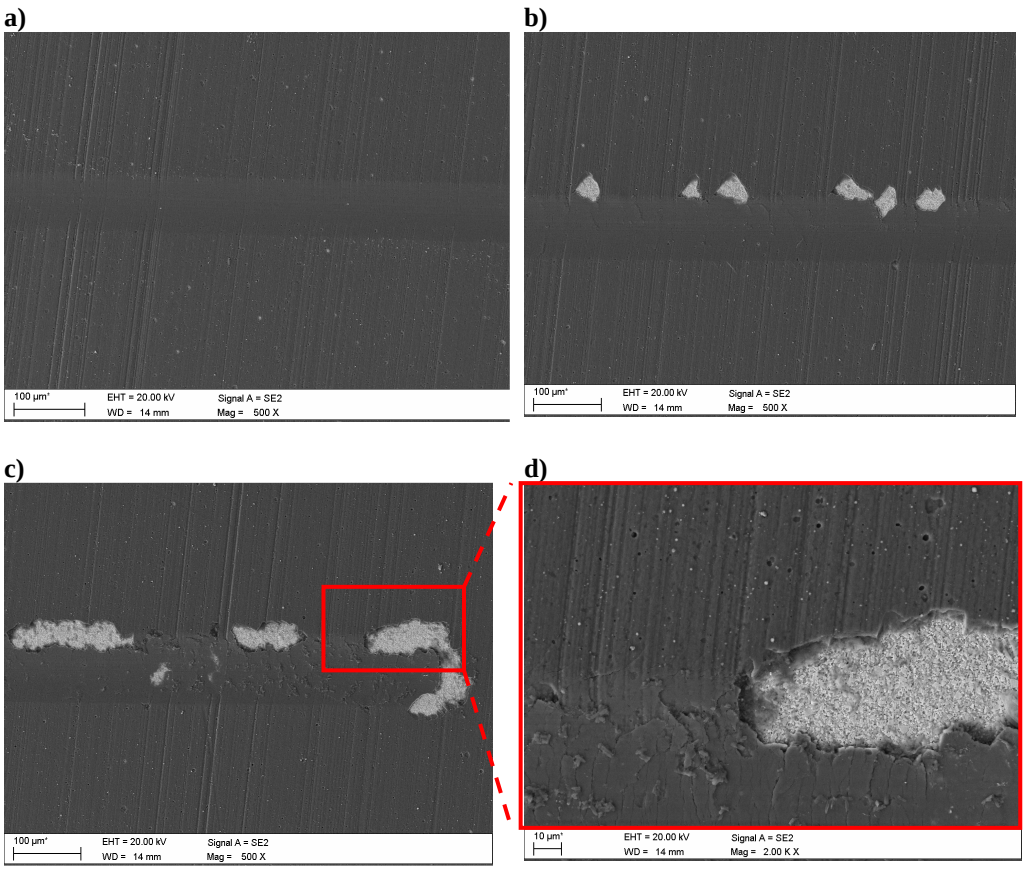

Figure 32. *a,b,c,d) Characteristic failure obtained by scratch test of the (Ti,Al)N coating deposited on cemented carbides substrate*

In the case of Ti(C,N) coatings we can observe the rise of tensile eigen-stresses in the contact area after the replacement of the single-layer coating with the gradient one (Table 3-4). In spite of this, higher adhesion has been demonstrated in the case of gradient Ti(C,N) coatings than in the case of respective single-layer coatings. It can be connected with the character of surface topography and the size of coating grains with respect to the roughness of the substrate, which, combined with the presence of tensile stresses, can result within certain limits in the positive influence of such stresses on the adhesion due to anchoring of the coating in a relevantly developed surface of the substrate [11].

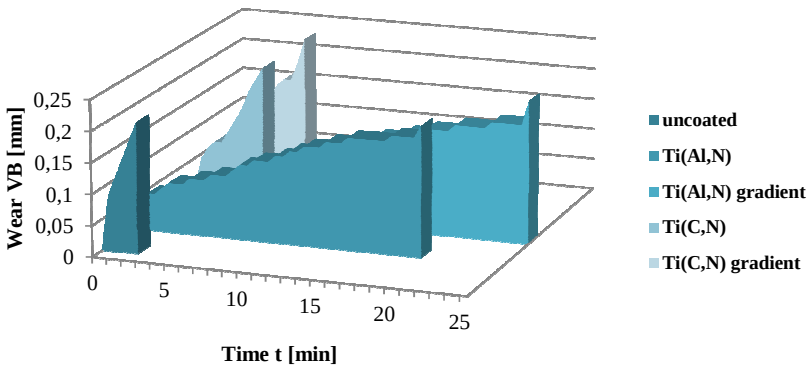

Figure 33. *Comparison of the approximated values of the VB wear of the cemented carbides sample: uncoated and coated with the PVD coatings, depending on machining time*

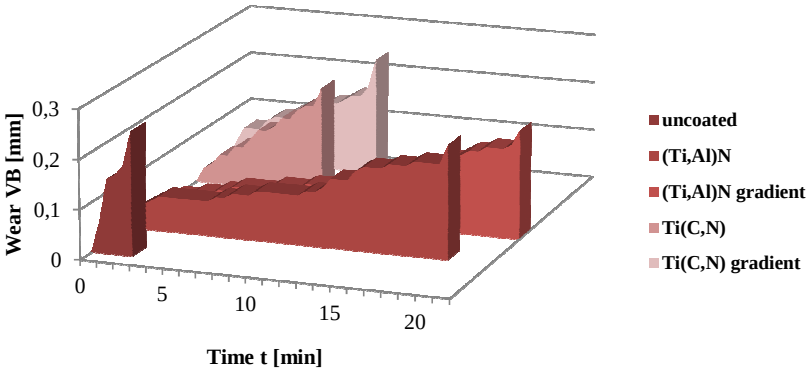

Figure 34. *Comparison of the approximated values of the VB wear of the cermets sample: uncoated and coated with the PVD coatings, depending on machining time*

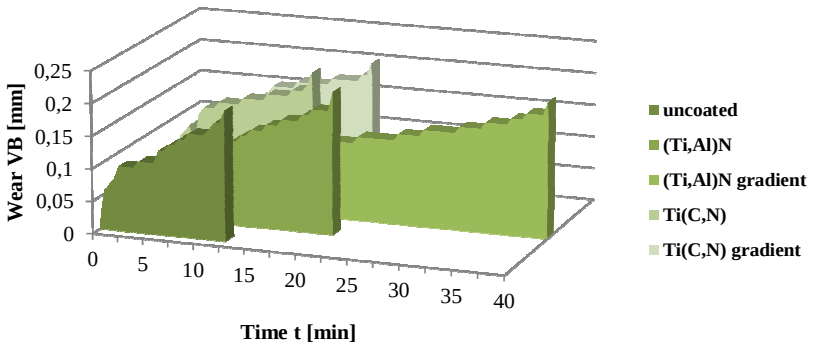

Figure 35. *Comparison of the approximated values of the VB wear of the Al_2O_3+TiC oxide tool ceramics sample: uncoated and coated with the PVD coatings, depending on machining time*

Due to the application of gradient coatings on all investigated substrate materials, we obtained compressive stresses in the surface layer of the coating having a direct contact with the machined material during the operation process (Table 3). In the case of gradient (Ti,Al)N coatings, we can observe a considerable rise of compressive stresses on the coating surface as compared to single-layer coatings (Table 3). In the case of Ti(C,N) coatings we can observe the change in the character of stresses on the coating surface from tensile stresses ,occurring on the surface of single-layer coatings, to compressive stresses occurring on the surface of gradient coatings. The generation of compressive stresses in the surface layer brings about better resistance to cracking, and through the rise of hardness, improves the wear resistance. The generation of compressive stresses in the surface layer can prevent the formation of cracks when the element in the operational conditions is subjected to stresses generated by external forces. Yet, an excessive value of compressive stresses can lead to adhesive wear and can bring about the formation of too high tensile stresses under the coating, lowering the fatigue resistance of the element [61,68]. Volvoda [67] pointed out the relation between the value of stresses and the hardness of the layer of titanium nitrides obtained in effect of magnetron sputtering, demonstrating that with the rise of compressive stresses the hardness of the obtained layer is progressively increasing. Basing on the carried out research, it was demonstrated that the occurrence of compressive stresses on the surface of gradient coatings of the investigated materials has a positive influence on their mechanical properties, in particular on the microhardness (Table 1).

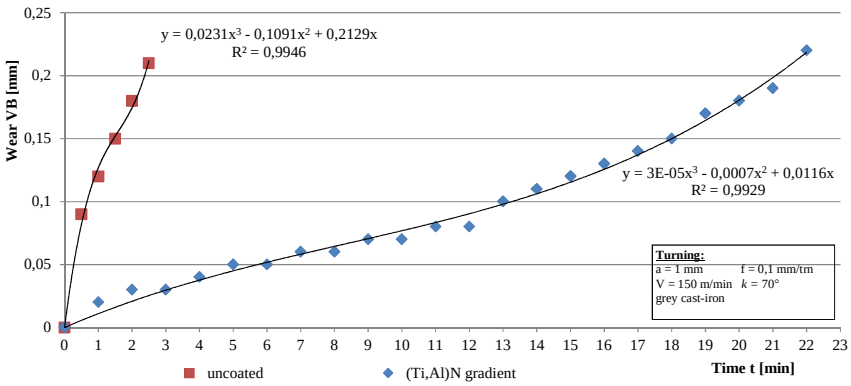

Figure 36. *Comparison of the approximated values of the VB wear of the cermets sample: uncoated and coated with the (Ti,Al)N gradient coating, depending on machining time*

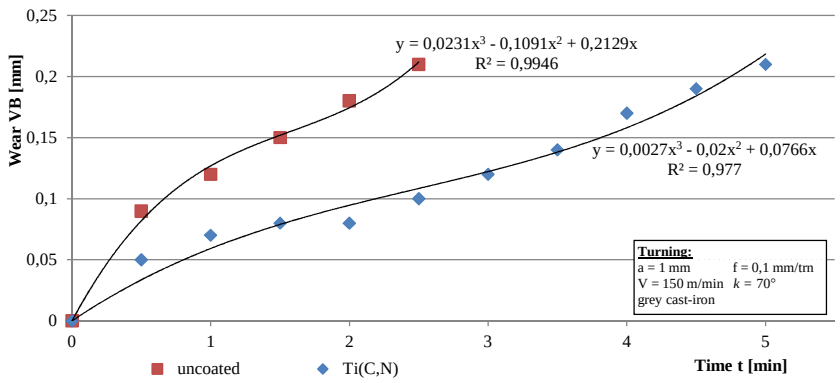

Figure 37. *Comparison of the approximated values of the VB wear of the cemented carbides sample: uncoated and coated with the Ti(C,N) coating, depending on machining time*

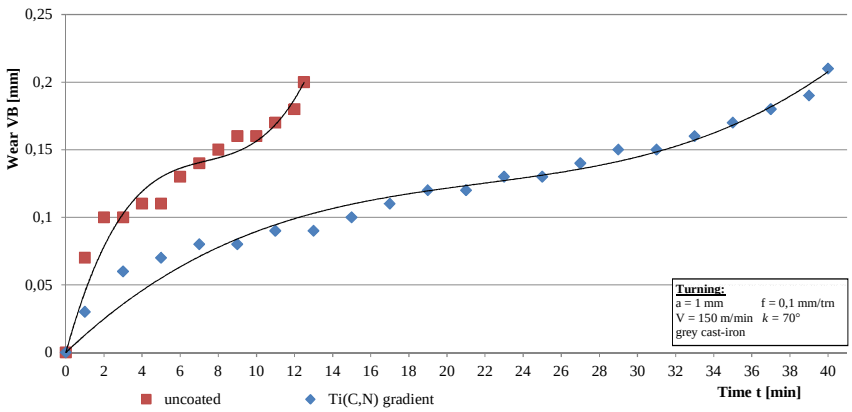

Figure 38. *Comparison of the approximated values of the VB wear of the Al_2O_3+TiC oxide tool ceramics sample: uncoated and coated with the Ti(C,N) gradient coating, depending on machining time*

Table 4. *Results of computer simulation of internal stresses in the analysed single-layer PVD coatings*

Substrate	Coating	Computer simulation results of internal stress, [MPa]
Cemented carbide	(Ti,Al)N	170
	Ti(C,N)	150
Cermet	(Ti,Al)N	-410
	Ti(C,N)	15
Al_2O_3+TiC	(Ti,Al)N	-180
	Ti(C,N)	150

Figure 40 present schematic distribution of stresses in the gradient coating (Ti,Al)N deposited on cemented carbide obtained by computer simulation

To verify the results of computer simulation, the values of eigen-stresses in the investigated single-layer and gradient coatings were calculated using the X-ray $\sin^2\psi$ technique (Table 5).

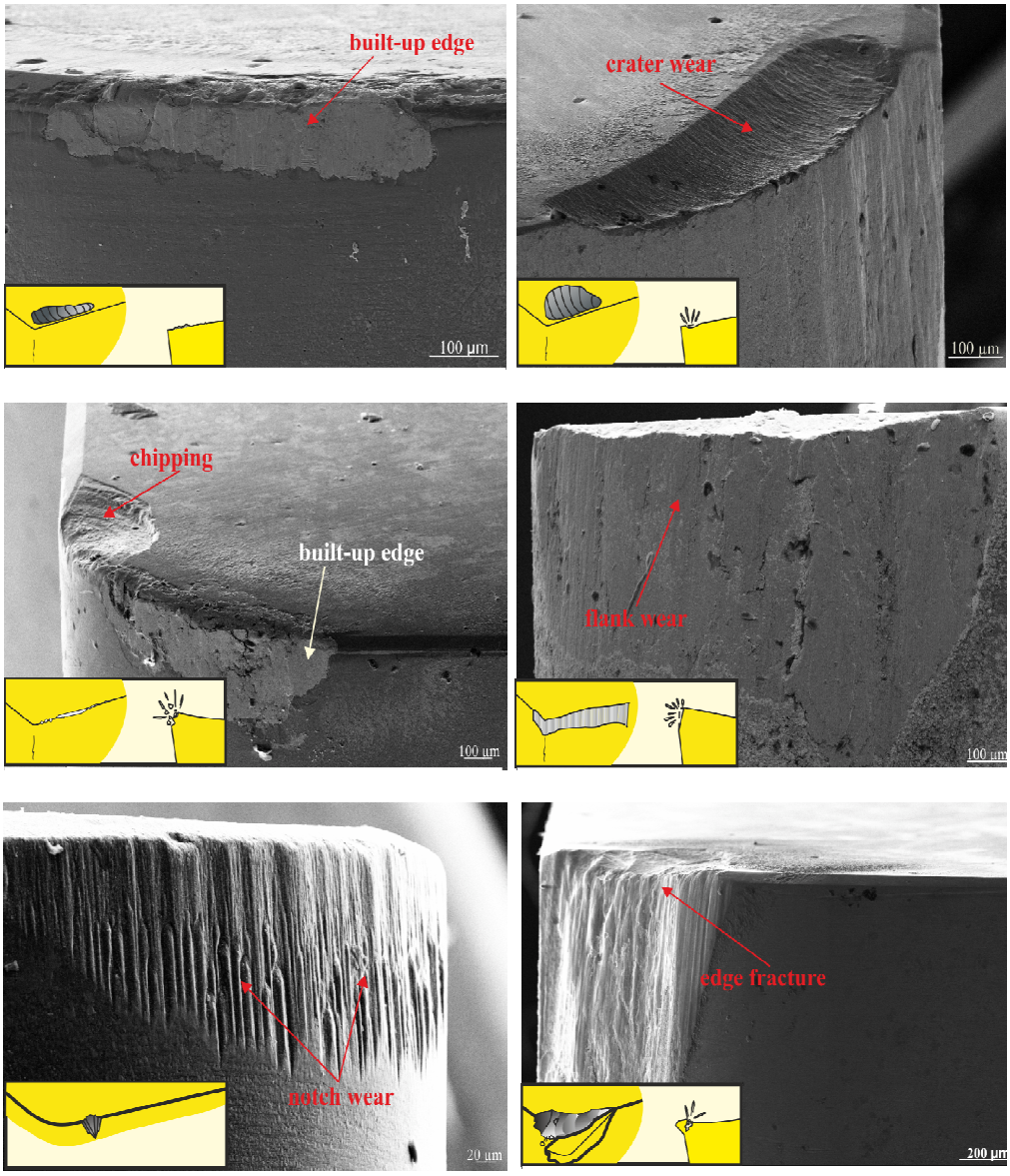

Figure 39. *Classification of character of tool wear of the sintered tool materials uncoated and coated with PVD coatings*

Table 5. *Results of experimental internal stresses using the X-ray $\sin^2\psi$ technique of the analysed PVD coatings*

Substate	Coating	Internal stresses, σ [MPa]
Cemented carbide	(Ti,Al)N	212±42
	(Ti,Al)N gradient	-395±45
	Ti(C,N)	-
	Ti(C,N) gradient	-
Cermet	(Ti,Al)N	-459±49
	(Ti,Al)N gradient	-647±77
	Ti(C,N)	-
	Ti(C,N) gradient	-
Al_2O_3+TiC	(Ti,Al)N	-228±48
	(Ti,Al)N gradient	-456±76
	Ti(C,N)	122±52
	Ti(C,N) gradient	-235±65

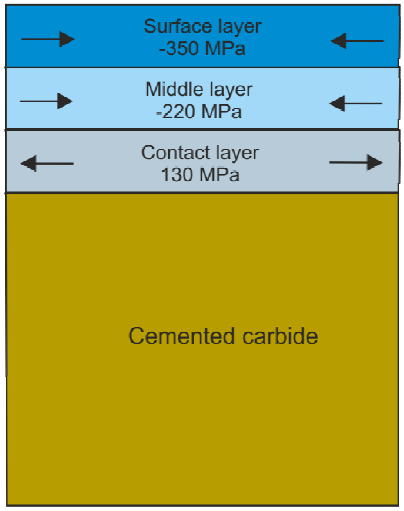

Figure 40. *Schematic distribution of stresses in the gradient coating (Ti,Al)N deposited on cemented carbide obtained by computer simulation*

4. Conclusions

The main objective of the work was to investigate the structure and properties of sintered tool materials, including cemented carbides, cermets and oxide ceramics deposited with single-layer and gradient coatings (Ti,A1)N and Ti(C,N), and to determine the relation between substrate type, coating material and linear variability of the chemical composition of the coating and the structure and properties of the obtained tool material (Fig. 41).

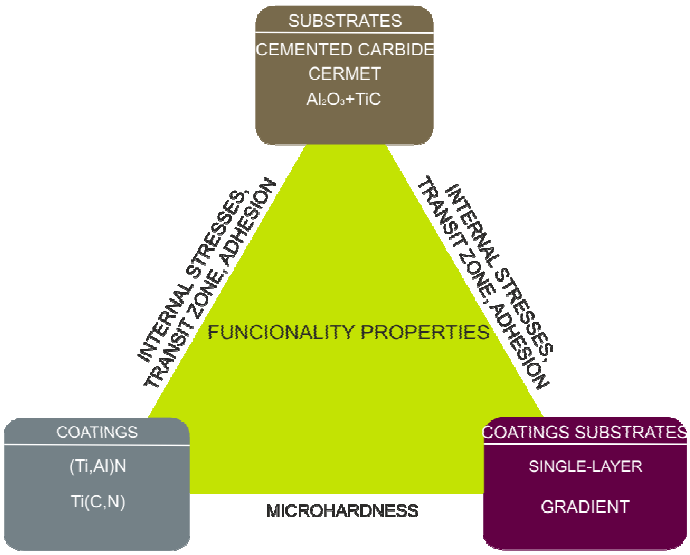

Figure 41. *Schematic diagram of the objective of the work*

Basing on the analysis of the obtained research results the following conclusions can be demonstrated:

1. The fabrication of PVD coatings of the type (Ti,Al)N and Ti(C,N) of the gradient structure and variable concentration of the components on the tools from sintered tool materials results in a considerable rise of applicability properties of tools produced in this way as compared to the tools deposited with a single-layer PVD coating or non-deposited coatings.
2. Gradient coatings are characterized by a linear change of chemical composition in the direction from the substrate to the coating surface. The deposited coatings demonstrate good and uniform adhesion to the substrate material and are characterized by column, fine-grained structure. In the contact area from the surface of the coatings we can observe a rise in the concentration of chemical elements being the components of the substrate, with a simultaneous decrease of the concentration of chemical elements forming these coatings, which can bespeak of the presence of a transit zone between the substrate material and coating.
3. A more advantageous distribution of stresses in gradient coatings than in respective single-layer coatings yields better mechanical properties, and, in particular, the distribution of stresses on the coating surface has the influence on microhardness, and the distribution of

stresses in the contact area between the coating and substrate has the influence on the adhesion of coatings.

4. The wear resistant gradient coatings of the type (Ti,Al)N and Ti(C,N) deposited on the investigated sintered tool materials yield a considerable rise of microhardness in the area around the surface, which, combined with good adhesion of the coating to the substrate obtained in effect of the application of gradient structure of the coating, has the influence on the applicability properties of these materials during machining tests, since the deposition of both single-layer and gradient coatings of the (Ti,Al)N type results in the rise of cutting edge durability as compared to the tools deposited with Ti(C,N) coatings. It is connected with high wear resistance of the (Ti,Al)N coating in raised temperature. It was also demonstrated that independent of the applied substrate type, higher wear resistance is exhibited by the materials deposited with gradient coatings as compared to the materials deposited with single-layer coatings.

Acknowledgements

The paper has been realised in relation to the project POIG.01.01.01-00-023/08 entitled “Foresight of surface properties formation leading technologies of engineering materials and biomaterials” FORSURF, co-founded by the European Union from financial resources of European Regional Development Found and headed by Prof. L.A. Dobrzański.

INNOVATIVE ECONOMY
NATIONAL COHESION STRATEGY

FORSURF

EUROPEAN UNION
EUROPEAN REGIONAL
DEVELOPMENT FUND

References

1. M. Antonov, I. Hussainova, F. Sergejev, P. Kulu, A. Gregor, Assessment of gradient and nanogradient PVD coatings behaviour under erosive, abrasive and impact wear conditions, Wear 267 (2009) 898-906.
2. M. Arndt, T. Kacsich, Performance of new AlTiN coatings in dry and high speed cutting, Surface and Coatings Technology 163-164 (2003) 674-680.
3. M.A. Baker, S.J. Greaves, E. Wendler, V. Fox, A comparison of in situ polishing and ion beam sputtering as surface preparation methods for XPS analysis of PVD coatings, Thin Solid Films 377-378 (2000) 473-477.

4. M. Bizjak, A. Zalar, P. Panjan, B. Zorko, B. Pracek, Characterization of iron oxide layers using Auger electron spectroscopy, Applied Surface Science 253 (2007) 3977-3981.
5. Y.Y. Chang, D.Y. Wang, Characterization of nanocrystalline AlTiN coatings synthesized by a cathodic-arc deposition process, Surface and Coatings Technology 201 (2007) 6699-6701.
6. J. R.C.Jr, Chastain, Handbook of X-ray Photoelectron Spectroscopy, Physical Electronics, Inc., 1995.
7. A.R. Chourasia, D.R. Chopra, Auger Electron Spectroscopy, Handbook of analytical chemistry, Prentice Hall, 1997.
8. M. Cłapa, D. Batory, Improving adhesion and wear resistance of carbon coatings using Ti:C gradient layers, Journal of Achievements in Materials and Manufacturing Engineering 20 (2007) 415-418.
9. G.E. D'Errico, R. Calzavarini, B. Vicenzi, Influences of PVD coatings on cermet tool life in continuous and interrupted turning, Journal of Materials Processing Technology 78 (1998) 53-58.
10. A. Demirkiran, E. Avci, Evaluation of functionally gradient coatings produced by plasma-spray technique, Surface and Coatings Technology 116-119 (1999) 292-295.
11. L.A. Dobrzański, Structure and properties of high-speed steels with wear resistant cases or coatings, Journal of Materials Processing Technology 109 (2001) 44-51.
12. K. Dybowski, Ł. Kaczmarek, R. Pietrasik, J. Smolik, Ł. Kołodziejczyk, D. Batory, M. Gzik, M. Stegliński, Influence of chemical heat treatment on the mechanical properties of paper knife-edge die, Journal of Achievements in Materials and Manufacturing Engineering 37/2 (2009) 422-427.
13. W. Kaczorowski, D. Batory, Carbon and titanium based layers for wood-based materials, Journal of Achievements in Materials and Manufacturing Engineering 27/2 (2008) 187-190.
14. B.G. Wndler, W. Pawlak, Low friction and wear resistant coating systems on Ti6Al4V alloy, Journal of Achievements in Materials and Manufacturing Engineering 26/2 (2008) 207-210.
15. M. Richert, A. Mazurkiewicz, J. Smolik, Chromium carbide coatings obtained by the hybrid PVD methods, Journal of Achievements in Materials and Manufacturing Engineering 43/1 (2010) 145-152.
16. L.A. Dobrzański, K. Gołombek, J. Mikuła, D. Pakuła, L.W. Żukowska, Sintered tools materials with multicomponent PVD gradient coating, Journal of Achievements in Materials and Manufacturing Engineering 31 (2008) 15-22.
17. J. Grabarczyk, D. Batory, P Louda, P. Couvrat, I. Kotela, K. Bakowicz-Mitura, Carbon coatings for medical implants, Journal of Achievements in Materials and Manufacturing Engineering 20 (2007) 107-111.
18. Z. Rożek, W. Kaczorowski, D. Lukáš, P. Louda, S. Mitura, Potential applications of nanofiber textile covered by carbon coatings, Journal of Achievements in Materials and Manufacturing Engineering 27/1 (2008) 35-38.
19. R.M. Nowak, S. Jonas, S. Zimowski, K. Tkacz-Śmiech, Amorphous carbon layers on polymeric substrates, Journal of Achievements in Materials and Manufacturing Engineering 25/1 (2007) 23-26.

20. B. Wendler, T. Moskalewicz, I. Progalskiy, W. Pawlak, M. Makówka, K. Włodarczyk, P. Nolbrzak, A. Czyrska-Filemonowicz, A. Rylski, Hard and superhard nanolaminate and nanocomposite coatings for machine elements based on Ti6Al4V alloy, Journal of Achievements in Materials and Manufacturing Engineering 43/1 (2010) 455-462.
21. W. Pawlak, B. Wendler, Multilayer, hybrid PVD coatings on Ti6Al4V titanium alloy, Journal of Achievements in Materials and Manufacturing Engineering 37/2 (2009) 660-667.
22. D. Batory, A. Stanishevsky, W. Kaczorowski, The effect of deposition parameters on the properties of gradient a-C:H/Ti layers, Journal of Achievements in Materials and Manufacturing Engineering 37/2 (2009) 381-386.
23. K. Włodarczyk, M. Makówka, P. Nolbrzak, B. Wendler, Low friction and wear resistant nanocomposite nc-MeC/a-C and nc-MeC/a-C:H coatimgs, Journal of Achievements in Materials and Manufacturing Engineering 37/2 (2009) 364-360.
24. W. Kaczorowski, D. Batory, P. Niedzielski, Application of microwave/radio frequency and radio frequency/magnetron sputtering techniques in polyurethane surface modification, Journal of Achievements in Materials and Manufacturing Engineering 37/2 (2009) 286-291.
25. W. Kwaśny, Predicting properties of PVD and CVD coatings based on fractal quantities describing their surface, Journal of Achievements in Materials and Manufacturing Engineering 37/2 (2009) 125-192.
26. W. Grzesik, Z. Zalisz, S. Król, Tribological behaviour of TiAlN coated carbides in dry sliding tests, Journal of Achievements in Materials and Manufacturing Engineering 17 (2006) 279-282.
27. G. Matula, Influence of binder composition on structure and properties of carbide alloyed composite manufactured with the PIM method, Journal of Achievements in Materials and Manufacturing Engineering 30/2 (2008) 193-196.
28. W. Kwaśny, A modification of the method for determination of the surface fractal dimension and multifractal analysis, Journal of Achievements in Materials and Manufacturing Engineering 33 (2009) 115-125.
29. L.A. Dobrzański, M. Staszuk, J. Konieczny, W. Kwaśny, M. Pawlyta, Structure of TiBN coatings deposited onto cemented carbides and sialon tool ceramics, Archives of Materials Science and Engineering 38/1 (2009) 48-54.
30. L.A. Dobrzański, M. Staszuk, J. Konieczny, J. Lelątko, Structure of gradient coatings deposited by CAE-PVD techniques, Journal of Achievements in Materials and Manufacturing Engineering 24/2 (2007) 55-58.
31. L.A. Dobrzański, L. Wosińska, K. Gołombek, J. Mikuła, Structure of multicomponent and gradient PVD coatings deposited on sintered tool materials, Journal of Achievements in Materials and Manufacturing Engineering 20 (2007) 99-102.
32. L.A. Dobrzański, L.W. Wosińska, J. Mikuła, K. Gołombek, T. Gawarecki, Investigation of hard gradient PVD (Ti,Al,Si)N coating, Journal of Achievements in Materials and Manufacturing Engineering 24 (2007) 59-62.

33. L.A. Dobrzański, L.W. Wosińska, J. Mikuła, K. Gołombek, D. Pakuła, M. Pancielejko, Structure and mechanical properties of gradient PVD coatings, Journal of Materials Processing Technology 201(2008) 310-314.
34. L.A. Dobrzański, L.W. Wosińska, J. Mikuła, K. Gołombek, Multicomponent and gradient PVD coatings deposited on the sintered tool materials, Materials Science 3-4 (157-158) (2007) 627-630.
35. L.A. Dobrzański, L.W. Żukowska, Properties of the multicomponent and gradient PVD coatings, Archives of Materials Science and Engineering 28/10 (2007) 621-624.
36. L.A. Dobrzański, L.W. Żukowska, W. Kwaśny, J. Mikuła, K. Gołombek, Ti(C,N) and (Ti,Al)N hard wear resistant coatings, Journal of Achievements in Materials and Manufacturing Engineering 42/2 (2010) 93-103.
37. L.A. Dobrzański, L.W. Żukowska, J. Mikuła, K. Gołombek, T. Gawarecki, Hard gradient (Ti,Al,Si)N coating deposited on composite tool materials, Archives of Materials Science and Engineering 36/2 (2009) 69-754.
38. L.A. Dobrzański, L.W. Żukowska, J. Mikuła, K. Gołombek, P. Podstawski, Functional properties of the sintered tool materials with (Ti,Al)N coating, Journal of Achievements in Materials and Manufacturing Engineering 36/2 (2009) 134-141.
39. L.A. Dobrzański, L.W. Żukowska, J. Kubacki, K. Gołombek, J. Mikuła, XPS and AES analysis of PVD coatings, Journal of Achievements in Materials and Manufacturing Engineering 32 (2008) 99-102.
40. J. Gu, G. Barber, S. Tung, R.J. Gu, Tool life and wear mechanism of uncoated and coated milling inserts, Wear 225-229 (1999) 273-284.
41. Y.H. Guu, H. Hocheng, Improvement of fatigue life of electrical discharge machined AISI D2 tool steel by TiN coating, Materials Science and Engineering A 318 (2001) 155-162.
42. J. Kopač, Influence of cutting materials and coating on tool quality and tool life, Journal of Materials Processing Technology 78 (1998) 95-103.
43. R. Kosiba, J. Liday, G. Ecke, O. Ambacher, J. Breza, P. Vogrincic, Quantitative Auger electron spectroscopy of SiC, Vacuum 80 (2006) 990-995.
44. J.H. Lee, S.J. Lee, One-step-ahead prediction of flank wear using cutting force, International Journal of Machine Tools and Manufacture 39 (1999) 1747-1760.
45. W. Lengauer, K. Dreyer, Functionally graded hardmetals, Journal of Alloys and Compounds 338 (2002) 194-212.
46. Li Chen, S.Q. Wang, Yong Du, Jia Li, Microstructure and mechanical properties of gradient Ti(C, N) and TiN/Ti(C, N) multilayer PVD coatings, Materials Science and Engineering A 478 (2008) 336-339.
47. C.Y.H. Lim, S.C. Lim, K.S. Lee, Wear of TiC-coated carbide tools in dry turning, Wear 225-229 (1999) 354-367.
48. C.H. Lin, J.G. Duh, J.W. Yeh, Multi-component nitride coatings derived from Ti-Al-Cr-Si-V target in RF magnetron sputter, Surface and Coatings Technology 201 (2007) 6304-6308.

49. T. Liu, C. Dong, S. Wu, K. Tang, J. Wang, J. Jia, TiN, TiN gradient and Ti/TiN multi-layer protective coatings on Uranium, Surface and Coating Technology 201 (2007) 6737-6741.
50. Y.H. Lu, Z.F. Zhou, P. Sit, Y.G. Shen, K.Y. Li, Haydn Chen, X-Ray photoelectron spectroscopy characterization of reactively sputtered Ti-B-N thin films, Surface & Coatings Technology 187 (2004) 98-105.
51. S.J. Skrzypek, W. Ratuszek, A. Bunsch, M. Witkowska, J. Kowalska, M. Goły, K. Chruściel, Crystallographic texture and anisotropy of electrolytic deposited copper coating analysis, Journal of Achievements in Materials and Manufacturing Engineering 43/1 (2010) 264-268.
52. S. Carvalho, E. Ribeiro, L. Rebouta, C. Tavares, J.P. Mendonca, A. Caetano Monteiro, N.J.M. Carvalho, J.Th. M. De Hosson, A. Cavaleiro, Microstructure, mechanical properties and cutting performance of superhard (Ti,SiAl)N nanocomposite films grown by d.c. reactive magnetron sputtering, Surface and Coatings Technology 177-178 (2004) 459-468.
53. R. Manaila, A. Devenyi, D. Biro, L. David, P.B. Barna, A. Kovacs, Multilayer TiAlN coatings with composition gradient, Surface and Coatings Technology, 151-152 (2002) 21-25.
54. G. Matula, Study on steel matrix composites with (Ti,Al)N gradient PVD coatings, Journal of Achievements in Materials and Manufacturing Engineering 34/1 (2009) 79-86.
55. P.H. Mayrhofer, Ch. Mitterer, L. Hultman, H. Clemens, Microstructural design of hard coatings, Progress in Materials Science 51 (2006) 1032-1114.
56. S. Mitura, A. Mitura, P. Niedzielski, P. Couvrat, Nanocrystalline Diamond Coatings, Chaos, Solitons& Fractals 10/12 (1999) 2165-2176.
57. Y. Miyamoto, W.A. Kaysser, B.H. Rabin, A. Kawasaki, R.G. Ford, Funcionally Graded Materials: Design, Processing and Applications, Kulwer Academic Publishers, Boston-Dordrecht-London 1999.
58. S. PalDey, S.C. Deevi, Cathodic arc deposited FeAl coatings: properties and oxidation characteristics, Materials Science and Engineering A355 (2003) 208-215.
59. S. PalDey, S.C. Deevi, Properties of single layer and gradient (Ti,Al)N coatings, Materials Science and Engineering A361 (2003) 1-8.
60. S. PalDey, S.C. Deevi, Single layer and multilayer wear resistant coatings of (Ti,Al)N: a review, Materials Science and Engineering A342 (2003) 59-79.
61. A. Perry, J.A. Sue, P.J. Martin, Practical measurement of the residual stress in coatings, Surface and coatings Technology 81 (1996)17-28.
62. X. Qiao, Y. Hou, Y. Wu, J. Chen, Study on functionally gradient coatings of Ti-Al-N, Surface and Coatings Technology 131 (2000) 462-464.
63. Catalogue, Sandvik-Coromant.
64. D. Rafaja, A. Poklad, V. Klemm, G. Schreiber, D. Heger, M. Sima, M. Dopita, Some consequences of the partial crystallographic coherence between nanocrystalline domains in Ti-Al-N and Ti-Al-Si-N coatings, Thin Solid Films 514 (2006) 240-249.

65. B. Navinsek, P. Panjan, I. Milosev, PVD coatings as an environmentally clean alternative to electroplating and electroless processes, Surface and Coatings Technology 116-119 (1999) 476-487.
66. A. Śliwa, J. Mikuła, K. Gołombek, L.A. Dobrzański, FEM modelling of internal stresses in PVD coated FGM, Journal of Achievements in Materials and Manufacturing Engineering 36/1 (2009) 71-78.
67. V. Volvoda: Structure of thin films of titanium nitride, Journal of Alloys and Compounds 219 (1995) 83-87.
68. U. Welzel, J. Ligot, P. Lamparter, Stress analysis of polycrystalline thin films and surface regions by X-ray diffraction, Applied Crystallography 38 (2005) 1-29.
69. I.Yu. Konyashin, PVD/CVD technology for coating cemented carbides, Surface and Coatings Technology 71 (1995) 277-283.

The paper is published also in the Journal of Achievements in Materials and Manufacturing Engineering